Review

Enzyme–Iron Oxide Nanoassemblies: A Review of Immobilization and Biocatalytic Applications

Ángeles Valls-Chivas [1,2,3,4], Javier Gómez [5], Jose I. Garcia-Peiro [1,2,3], Felipe Hornos [1,5,*]
and Jose L. Hueso [1,2,3,4,*]

[1]   Instituto de Nanociencia y Materiales de Aragón (INMA), CSIC-Universidad de Zaragoza, Campus Rio Ebro, Edificio I+D, C/Poeta Mariano Esquillor, s/n, 50018 Zaragoza, Spain
[2]   Department of Chemical and Environmental Engineering, University of Zaragoza, Campus Rio Ebro, C/María de Luna, 3, 50018 Zaragoza, Spain
[3]   Networking Research Center in Biomaterials, Bioengineering and Nanomedicine (CIBER-BBN), Instituto de Salud Carlos III, 28029 Madrid, Spain
[4]   Instituto de Investigación Sanitaria (IIS) de Aragón, Avenida San Juan Bosco, 13, 50009 Zaragoza, Spain
[5]   Instituto de Investigación, Desarrollo e Innovación en Biotecnología Sanitaria de Elche (IDiBE), Universidad Miguel Hernández, 03202 Elche, Spain
*   Correspondence: fhornos@umh.es (F.H.); jlhueso@unizar.es (J.L.H.)

Abstract: In the search for new biotechnological advances, increasing attention is currently being paid to the development of magnetic nanoplatforms loaded with enzymes, since, on the one hand, they can be recovered and reused, and on the other hand, they improve their catalytic activity and increase their stability, avoiding processes such as aggregation or autolysis. In this review, we evaluate a series of key parameters governing the enzyme–nanoparticle immobilization phenomena from a thermodynamic and kinetic point of view. We also focus on the use of magnetite nanoparticles (MNPs) as multifunctional vectors able to anchor enzymes, summarize the most relevant aspects of functionalization and immobilization and, finally, describe some recent and relevant applications of the enzyme–MNP hybrids as biocatalysts with especial emphasis on cancer therapy.

Keywords: enzyme adsorption; magnetic nanoparticles; enzymatic activity; coating; polyelectrolytes; nanomedicine; nanobiotechnology; hybrids; composites; immobilization

1. Introduction

Enzymes are biomolecules of paramount importance for the correct functioning of any biological system. They act as catalysts for multiple reactions involved in cell metabolism [1]. These enzymes exhibit remarkable advantages, such as high catalytic activity and high substrate specificity. Recent advances in biotechnological processes have promoted the use of enzymes for the development of a wide plethora of environmental, industrial and biomedical applications [2–5]. In the biomedical field, there exists an urgent need to immobilize the enzymes in order to maximize their efficient delivery into the tumor microenvironment (TME) [6,7]. Their selective catalytic response can be useful as an alternative to non-specific conventional treatments such as chemotherapy or radiotherapy. It may also represent an appealing complement to emerging therapies such as photothermal, photodynamic, immunotherapy, chemodynamic or starvation therapy [8–12].

The immobilization of enzymes to both hydrophilic and hydrophobic surfaces responds to their amphipathic nature [3,5,13–29]. This behavior has been profusely used in applications such as chromatographic separation [30], the development of new encapsulation and transport systems [31,32], sensors [33] or new biocompatible materials or hybrid robots [19,20,34–38]. However, undesired adsorption of enzymes and other biomolecules to solid surfaces often leads to a decrease in their conformational stability [39–41] or structural and functional changes potentially causing negative effects [42]. Examples of these processes

include adsorption of enzymes on solid glass and plastic surfaces or contact lenses [43], inducing a certain loss of activity. Enzyme aggregation processes may also lead to the development of thrombi in artificial implants and potential immunogenicity [41,44–46].
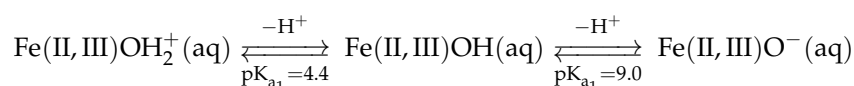
Functionalized magnetic nanoparticles (MNPs) hold a great potential as potential nanoplatforms that can help to immobilize enzymes, prevent their inactivation and, most importantly, maximize their reuse and recovery [28,47–49]. The use of different molecules for their functionalization depends on both the enzyme to be immobilized and the desired therapeutic use [48,50]. This represents an important economic advantage in the biotechnology industry. A field with potential development, and which adds advantages over the use of magnetic nanoparticles versus non-magnetic nanoparticles, is the possibility of controlling the catalytic performance of the enzyme by increasing the local temperature upon application of an external electromagnetic stimuli [19,51–53]. In addition, their magnetic properties make them very versatile in the biomedical field since they can be used in hyperthermia and in diagnostics for magnetic resonance imaging (MRI). Furthermore, iron-based NPs may additionally perform chemodynamic therapy (CDT) which exploits the decomposition of overproduced H_2O_2 through a Fenton-like reaction catalyzed by the Fe atom of the magnetite nanoparticle to selectively induce apoptosis in cancer cells due to hydroxyl radical ($^\bullet$OH) generation [16,54–56]. The ROS generated through CDT can induce oxidative stress in cancer cells, leading to DNA damage, lipid peroxidation (i.e., ferroptosis) and other cellular damage to induce cell death. This redox ability also favors the synergistic combination with other relevant therapies such as photodynamic therapy, electrodynamic therapy, bioorthogonal catalysis or starvation therapy [16–18].

This review aims at highlighting the parameters governing the immobilization of enzymes onto nanoparticles, paying attention to the thermodynamics and the kinetics. It also describes the most extended functionalization strategies of magnetic nanoplatforms and, finally, we establish the main enzyme immobilization approaches while surveying the most relevant catalytic application of enzyme–MNPs reported in the recent literature for biotechnological and biocatalytic application with especial emphasis on cancer therapy.

2. Iron Oxide Magnetic Nanoplatforms

2.1. Stability and Coating Strategies

Due to this great property of nanoparticles, many applications have been generated, both at an industrial level for bioremediation [57] and catalysis [58], or at a biomedical level for magnetic resonance imaging (MRI) [59], hyperthermia [60] or drug delivery systems [9–12,16,61]. The poor stability of magnetite nanoparticles at a near physiological pH has, in recent decades, boosted their stabilization by coating their surface to increase their colloidal stability. To understand this limited colloidal stability of magnetite particles in an aqueous solution under physiological conditions, it is first necessary to explain the acid-base behavior of this iron oxide. There is now a consensus that, in the case of magnetite, this behavior is consistent with the existence of two proton dissociation equilibria to which two values of pKa can be ascribed, 4.4 and 9.0 [62].

$$\text{Fe(II, III)OH}_2^+ \text{(aq)} \underset{\text{pK}_{a_1}=4.4}{\overset{-\text{H}^+}{\rightleftarrows}} \text{Fe(II, III)OH(aq)} \underset{\text{pK}_{a_1}=9.0}{\overset{-\text{H}^+}{\rightleftarrows}} \text{Fe(II, III)O}^- \text{(aq)}$$

If we simulate the surface charge variation as a function of the pH, assuming the previously mentioned pKa values, we find that at pH 6.7, the net charge on the nanoparticle surface is zero (PZC, point of zero charge), being positive at a pH below the PZC and negative when above the PZC (Figure 1).
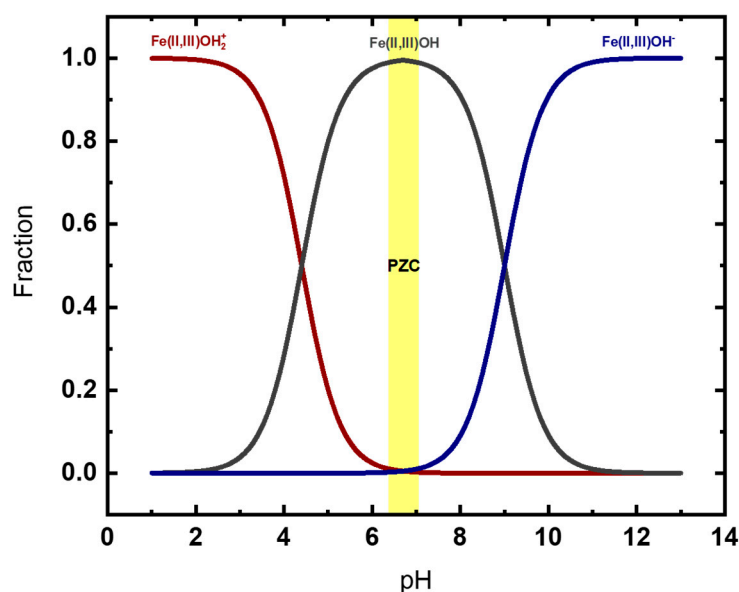
Figure 1. Expected variation in the fraction of each of the three species, Fe(II, III)OH$_2^+$, Fe(II, III)OH and Fe(II, III)O$^-$, as a function of pH with pKa values of 4.4 and 9.0. The yellow highlighted area represents the PZC.

Therefore, both at a low and high pH, the surface of the magnetite particles will be strongly positively or negatively charged. Under these conditions, a strong electrostatic repulsion will be established between them, increasing their colloidal stability, as this repulsion opposes their hydrophobic collapse, aggregation and consequent precipitation.

In contrast, as the pH of the solution approaches the PZC, the surface charge of the particles will decrease and, therefore, the electrostatic repulsion will weaken. This approach of the pH of the solution to the PZC of the nanoparticles will reduce their colloidal stability, making agglomeration and subsequent flocculation more likely. The stability of magnetite nanoparticles in the solution depends on the balance between attractive and repulsive forces as described by the DLVO theory developed by Derjaguin and Landau in 1941 and by Verwey and Overbeek in 1948, where the repulsive forces depend on the potential and thickness of the electrical double layer, the particle radius and the dielectric constant of the medium, while the attractive forces depend on van der Waals forces [63,64]. To achieve the stabilization of nanoparticles, we can use different methodologies based on the two types of repulsive forces (electrostatic or steric) whose effective repulsive force has to overcome the ever-present van der Waals forces of attraction [65]. For this purpose, different stabilizing molecules can be used to coat these nanoparticles [66] since, in addition to presenting magnetic capacity, their surface will show different functional groups depending on the type of treatment/coating that has been used (Figure 2).

The use of carboxylic acids, such as citric acid with pKa values of 3.13, 4.76 and 6.4, offers a high affinity as a chelating agent for Fe^{2+} and, especially, Fe^{3+} ions [67]. Because of this, at least one carboxylic group can be exposed to the solvent and, consequently, will impart a negative charge to the particle. This type of coating has been used to stabilize magnetite nanoparticles for further application in MRI [68] or bioimaging [69]. Oleic acid is an unsaturated fatty acid whose carboxylic acid has a pKa of 5.02 [67]. Although oleic acid is only soluble in non-polar solvents, when bound to magnetite nanoparticles, they can form a double layer if the pH is adjusted properly in polar solvents [68]. While nanoparticles can also be stabilized by forming a single oleic acid layer, these are only soluble in non-polar solvents and, therefore, may not show any use in biological applications [67]. Like citrate, the interaction of oleic acid with the surface is very strong, the interaction taking place via a carboxylate group. Following these protocols, nanoparticles stabilized by this double layer have been synthesized for applications such as hyperthermia or MRI, where they

determine that due to the coating, there is a loss in magnetization, but without losing the superparamagnetic capacity [69,70].
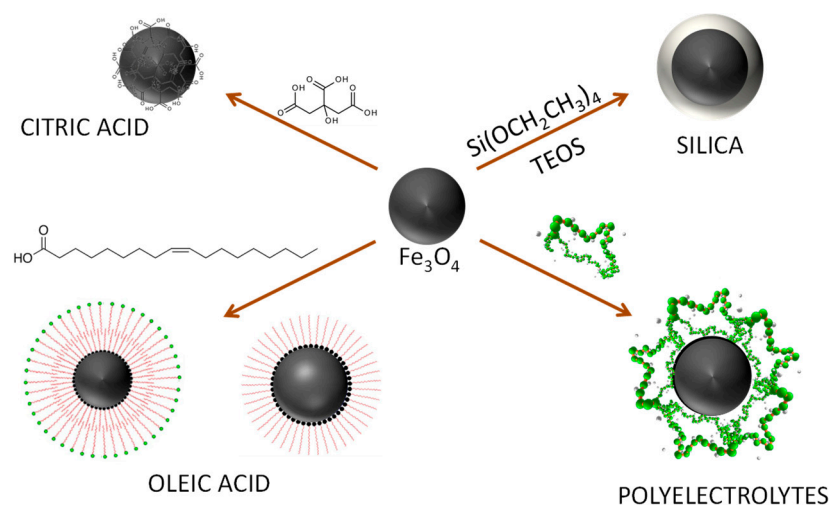

Figure 2. Schematic representation of the possible stabilization of magnetic nanoparticles with different substances.

The coating of nanoparticles with silica shells has significant advantages due to the stability of its covalent network. It provides a negative charge to the particle over a wide pH range. The pH at which the surface has a net zero charge is around 2–3 [71]. In turn, due to the deprotonation of the silanol groups, the negative charge density on the surface increases with the pH. Silica depolymerization occurs at a high pH (pH > 11), leading to dissolution of the coating [72]. Because of this, it is possible to prevent aggregation of the bare nanoparticle at the physiological pH. Another advantage is due to the silanol groups on its surface, which make it very reactive and easily derivatizable, being able to covalently bind different molecules [73,74]. It also makes the particle more compatible for biomedical applications [75–77].

Alternatively, a wide variety of neutral polymers or polyelectrolytes have been tested to stabilize magnetite nanoparticles, by in situ addition either during particle formation or by post-processing [78]. Dextran [79], chitosan [80], alginate [81], polyvinyl alcohol (PVA) [82], PEG [83] or PEI [84] appear among the most commonly used biocompatible polymers. Charged polymers have undoubtedly been the most widely used in the stabilization of magnetite particles because the resulting coating, in addition to significantly increasing their colloidal stability, allows for the adsorption of oppositely charged ligands. Polyelectrolytes are polymers containing ionizable groups which, in polar solvents, can dissociate into charged polymeric chains (macroions) and small counterions [85]. In the solution, these counterions are condensed on the polymer chain, according to the counterion condensation theory proposed by Manning in 1969 [86]. The charge density of the polyelectrolyte will depend on several factors: those intrinsic to the polyelectrolyte, such as the structure or type of ionizable group present, and those extrinsic to it, such as the nature and concentration of the counterion, ionic strength, pH or temperature [87,88]. An important aspect in polyelectrolyte conformation is the ionic strength since, in the absence of or low ionic strength, the polyelectrolyte adopts a "stretched" conformation since the charged groups repel each other, while at a high ionic strength, the polyelectrolyte adopts a "folded" conformation due to charge shielding, as stated by Kokufuta et al. [89] in their 1986 research.

2.2. Coated versus Non-Coated Magnetic Nanoparticles and Their Comparative Performance in Biocatalytic Applications

The literature available for the immobilization of enzymes on bare magnetite nanoparticles is scarce and somehow contradictory. Some authors claim that there is no efficient interaction between the support and the enzyme, in addition to the surface being susceptible to oxidation or acidic environments [5,90,91]. Still, some authors claim the use of bare nanoparticles to immobilize enzymes, as in the case of Roth H. C. et al. [92], where they immobilized, through an adsorption process, cellulase both on bare particles and on particles coated with silica. They argued that the mechanism in the adsorption process is different because the desorption enthalpy varies in both systems, 5 mW·mg^{-1} for the bare ones and 100 mW·mg^{-1} for the silica-coated ones. Although the amount of enzyme that is adsorbed is very similar, 0.37 and 0.43 g·g^{-1} for the bare and coated, respectively, the enzyme activity is half for the one that has been adsorbed on the bare nanoparticle (26 vs. 13 U·g^{-1}). Considering that the adsorbed amount differs by 14%, compared to 50% in activity, the enzyme is most probably denatured.

From a thermodynamic perspective, the adsorption process of enzymes onto charged solid/rigid surfaces should decrease the free energy of the system as the number of opposite charge contacts increases, since the process is entropically driven [48]. It is, therefore, foreseeable that the process will modify the conformational equilibrium of the enzyme toward more disordered states than the native ones (partially folded states), thereby establishing a greater number of attractive electrostatic contacts. In terms of morphology, the curvature and available surface area of the particles play a fundamental role in these conformational changes; as the surface area of the solid increases, there is a greater conformational change in the secondary structure, and the change in the tertiary structure does not increase [41,93]. On the other hand, the more curved the surface of the nanoparticle (which translates into a smaller size, assuming a spherical geometry), the greater the ability of the enzyme to adapt to this surface without paying an excessive price in terms of its conformational stability. As the particle size increases, its curvature decreases (becoming null for flat surfaces), and, therefore, the adsorption of the enzyme will favor more extended conformational states of the enzyme, decreasing its conformational stability.

In an attempt to mitigate adverse effects, polymers are often used to stabilize rigid nanoparticles, giving greater flexibility to the groups that remain in contact with the solution. Since the contact of the enzyme with the surface is now through these polymers, it is well known that they can stabilize the enzyme, either by non-ionic polymers or ionic polymers (as is the case of polyelectrolytes) [94,95]. In the case of PEI, it is known to be a good membrane-destabilizing agent in both eukaryotic and prokaryotic cells, favoring cell permeabilization [94,96]. In addition, it prevents the dissociation of multimeric enzymes, increasing their stability [84]. Many have used this coating to promote the adsorption of different enzymes, such as GOx, an enzyme that catalyzes the oxidation of glucose to gluconolactone, where they see that binding with PEI increases the thermal stability of the enzyme, going from 50 °C for the free enzyme up to 70 °C [95]. Other authors found that the enzyme lactate dehydrogenase with 10 mg·mL^{-1} PEI (*w/v*) protects the sulfhydryl groups against oxidation, preventing their aggregation when the enzyme is stored for 1 month at 36 °C [97]. In contrast, in the case of non-ionic polymers, it has been shown that using PEG increases the storage stability at 4 and 30 °C [98].

Singh V. et al. [99] immobilized xylanase on bare and silica-coated magnetite nanoparticles. In their work, they highlighted the importance of coating the surface with inert silica, since the coated nanoparticles are less prone to degradation and oxidation, so the immobilized enzyme showed a higher catalytic activity over a wide range of temperatures and pH, with respect to that immobilized on the bare nanoparticle. Nematian T. et al. [100] also performed a comparative study on lipase immobilization on graphene oxide-coated and uncoated nanoparticles. The loading capacity of the coated nanoparticle with respect to the uncoated one was almost threefold, 24 wt.% versus 70 wt.% of the coated one. Further-

more, from the kinetic parameters determined (K_{cat}/K_m), they concluded that the catalytic capacity of the enzyme increased when it was immobilized on the coated surface.

3. Enzyme Immobilization Process: A Thermodynamic and Kinetic Viewpoint

3.1. Enzyme Immobilization Strategies

The immobilization of enzymes on different supports arises from the need to reuse enzymes due to their high costs. This process has improved the catalytic capacity of the enzyme with respect to the free one, increasing its thermal stability after immobilization, as well as the pH range where it can be used [5,101]. The immobilization of the enzyme can be performed through an extensive number of methods, the most commonly used being adsorption, covalent bonding, encapsulation and cross-linking [13–15,27–29,102]. In the cross-linking method, enzymes are interconnected by means of a cross-linker, usually glutaraldehyde. This method originates enzyme aggregates or CLEAS (cross-linking enzyme aggregates), where multiple bonds are produced between different protein molecules, which can either stabilize the enzyme or, to a certain degree, cause partial denaturation, with its consequent loss of activity. In the last decade, these CLEAS have been combined with magnetite particles (mCLEAS), allowing for the rapid recovery of the reaction medium [5,90]. As for the encapsulation method, the enzyme is immobilized on a porous support. It has the great advantage of minimizing the release of the enzyme. However, it has some limitations, in that not just any support can be used and that there may be mass transfer problems [90,103]. In this regard, the use of mesoporous silica nanoplatforms can be an excellent alternative [104].

Focusing on magnetic nanomaterials, most of the works reported in the literature immobilize the enzyme via adsorption, either through establishing electrostatic interactions or covalent bonding. Additional and detailed reviews can be found in [5,25–28,49]. Of the 52 articles summarized in this review that immobilize enzymes on magnetic nanoparticles, 27 authors opted for covalent immobilization, 24 selected adsorption (3 of them by metal affinity) and 1 by encapsulation (probably due to the above-mentioned limitations). Since most authors use adsorption or covalent bonding, we focus the discussion on these two methods. Both strategies have pros and cons, and the isoelectric point of the selected enzyme must be taken into account for a successful immobilization outcome. When the immobilization is carried out electrostatically, by adsorption, there is the possibility that the enzyme is desorbed from the surface and, therefore, the enzyme charge on the nanoparticles decreases. This can have a detrimental effect, especially at the industrial level. To prevent desorption, covalent binding is often used. Nevertheless, the reagents for this purpose, such as NHS (N-ydroxysuccinimide)/EDC (N-(3-dimethylaminopropyl)-N′-ethylcarbodiimide hydrochloride), are very unstable in the solution, which may result in low enzyme binding [105], not to mention that this process can be more costly to perform, both procedurally and economically.

The adsorption process can be less invasive than the one used for covalent binding, since the enzyme will bind by those residues that present an opposite charge to the surface, maintaining certain flexibility, not forcing the enzyme to have to bind to the surface by certain amino acids as can be the case with covalent binding. Although in both cases, the enzyme may suffer conformational losses, covalent binding would be more detrimental, and may even force the enzyme to bind through the active site, thus deactivating its catalytic activity. This covalent binding to the enzyme usually takes place by the side chains of different amino acids, such as lysine, cysteine, aspartic or glutamic acids [106]. Other factors such as the pH or ionic strength actively influence the adsorption process. In the case of covalent bonding, both parameters do not affect the process. Perhaps, for applications where there is a strong change in the pH, differentiating between synthesis pH and working pH, we should opt for covalent immobilization, thus preventing the enzyme from desorbing. In the case of adsorption, the pH of use is more limited, and we can minimize the possible desorption of the enzyme on the surface, if prior adsorption is carried out at the ionic strength conditions at which we are going to use our system. For

biomedical applications, adsorption immobilization may be of more interest in some cases. In the TME, for example, the pH is usually more acidic than the physiological pH [107], so we could adsorb an enzyme at the physiological pH, design a system that reversibly alters the conformational state of the enzyme, transport it to the "inactive" TME and when it reaches the site, given the pH change, desorption of the enzyme occurs and, therefore, the activation of the same, with the consequent recovery of its catalytic capacity.

3.2. Thermodynamic Considerations in the Enzyme Adsorption Process

Enzyme adsorption can be defined as the spontaneous adhesion of one or several layers of enzyme (or biomolecules) on a surface, being driven by the decrease in free energy derived from both the establishment of favorable interactions (both electrostatic and hydrophobic) and the entropic increase induced by the dehydration of both the nanoparticle surface and the biomolecule itself (which involves the release of water molecules). Each enzyme has a unique composition and structure due to the different display of amino acids (up to 20 different ones). In addition, they exhibit different characteristics depending on their polarity, causing those that are non-polar to be mostly buried inside the enzyme, while the polar and charged ones are preferentially found on the surface of the enzyme, contributing favorably to their adsorption on surfaces of opposite charge [108].

This adsorption process can be characterized by the adsorption isotherm, which represents the amount of adsorbate (ligand adsorbed) per unit mass (or area) of adsorbent (material from which the solid nanoparticle is made) as a function of the concentration of ligand in the solution in equilibrium with the nanoparticle–ligand complex. The first adsorption isotherm was proposed by Langmuir in 1918 [109]. Although it was developed to describe the adsorption of gases to solid surfaces, it is frequently used to explain the adsorption of other ligands, in particular proteins, in sufficiently dilute dispersions [110]. Although there are several types of isotherms, the type I isotherm or Langmuir isotherm (Equation (1)) is the most widely used.

$$q = \frac{m_{enzyme}}{m_{NP}} = \frac{K \cdot [E]}{1 + K \cdot [E]} \cdot q_{max} = \frac{[E]}{K_D + [E]} \cdot q_{max} \tag{1}$$

where q is the mass of enzyme adsorbed per unit mass (or area) of nanoparticle, q_{max} is the maximum amount of enzyme adsorbed per unit mass (or area) of nanoparticle (once saturation is reached), [E] is the concentration of enzyme in the solution and K is the equilibrium constant of the adsorption process ($K_D = 1/K$, the dissociation constant).

Q increases monotonically and saturated with [E] (for a constant nanoparticle amount). As [E] increases, the increase in q becomes smaller, tending asymptotically to q_{max}, when the nanoparticle surface is completely coated with enzyme [108].

This adsorption model assumes that [111]:

- Only a monolayer is formed, i.e., only one molecule is bound per binding site.
- The surface is homogeneous, so all binding centers are identical.
- The binding sites are independent, i.e., the adsorption of one molecule does not affect the adsorption of the next molecule.
- There is no competition for binding sites.
- Adsorption is reversible.

From the Langmuir isotherm, we can obtain information about the affinity with which adsorption occurs (equilibrium constant, K), and the maximum adsorption capacity of the surface, q_{max}.

For heterogeneous surfaces with different binding sites, the Freundlich isotherm model can be applied [111] (Equation (2)), which shows a purely empirical relationship between the amount of adsorbate bound to the surface and its concentration in the solution, provided

that n > 1. It is also applied for systems that do not fit to the Langmuir isotherm [112], since saturation is not reached in this model.

$$q = K \cdot [E]^{1/n} \cdot q_{max} \tag{2}$$

where K and n are parameters that depend on the adsorbent surface and the characteristics of the adsorbate, [E] is the concentration of enzyme present in the solution in equilibrium with the surface and q, q_{max} represents the mass of enzyme adsorbed on the unit mass (or area) of the adsorbent (nanoparticle).

From the two previous isotherms, the Langmuir–Freundlich isotherm has been proposed (Equation (3)) [113] to unify both models.

$$q = \frac{K \cdot [E]^{1/n}}{1 + K \cdot [E]^{1/n}} \cdot q_{max} \tag{3}$$

In the isotherm plot, we can distinguish two regions; the initial part and the final region where surface saturation is reached. In the initial part, where the concentration of the enzyme in the solution is low, the percentage of surface area covered by the adsorbed enzyme molecules remains low. Thus, the adsorption energetics are described as the simple adsorption of enzyme molecules to the solid surface since the interactions between individual enzyme molecules on the surface are negligible.

There are numerous studies characterizing the adsorption of proteins or enzymes on magnetite nanoparticles. Most of them select the Langmuir model, since they obtain better results in the fit than the Freundlich model. Table 1 shows a summary of the characterization of the adsorption process by fits to the adsorption isotherm. The parameters that can be extracted from the fits, such as K_d or q_{max}, are used to compare the higher or lower selectivity of the synthesized support, as well as the affinity toward it. Ding C. et al. [114] synthesized Cu^{2+}-EDTA-Fe_3O_4 nanoparticles to remove hemoglobin in blood samples. After performing the adsorption isotherm, they fitted both the Langmuir and Freundlich models, showing better results for the first one. These nanoparticles showed a high efficiency, qmax of 1277 mg·g^{-1}, and excellent selectivity, since other proteins showed a much lower adsorption capacity, 311 for BSA and 192 for lysozyme. They concluded that the material exhibited great potential for removing His-rich proteins. Likewise, Wang J. et al. [115] also designed Fe_3O_4@ytterbium silicate microspheres with a hemoglobin selective capacity against other enzymes or proteins such as β-Lactogloagulin, Lysozyme, α-Lactalbumin, Bovine serum albumin and Fetuin. After making fits to the Langmuir isotherm, they obtained adsorption capacities, q_{max} of 304.4, ~75, ~60, ~50, ~45, ~32 mg·g^{-1}, respectively. Kamran S. et al. [116] synthesized some magnetite nanoparticles coated with ionic liquids, [C_4MIM], [C_6MIM] y [C_8MIM], on which they determined the adsorption capacity of lysozyme using the Langmuir isotherm model. The adsorption capacity of lysozyme increased with respect to the order of hydrophobicity of the ionic liquid, [C_8MIM] > [C_6MIM] > [C_4MIM]. On the other hand, the affinity toward the surface, K_d, remained very similar for the three ionic liquids, but was much higher than the nanoparticles that had not been coated.

From a thermodynamic point of view, what promotes adsorption? Both enthalpy and entropy contributions play an important role in this process, depending on the type of surface and enzyme (Table 2). In the following, a description will be given of the energetics of enzyme adsorption processes to both hydrophilic solid surfaces (where electrostatic and hydrogen bonding interactions are established) and hydrophobic ones (where dehydration of hydrophobic surfaces of the interacting species will play a crucial role in the adsorption energetics). There are many processes of enzyme adsorption to solid surfaces where an increase in the adsorption constant, K, with temperature has been demonstrated, suggesting a positive value (unfavorable for the variation in the free energy of adsorption) of the binding enthalpy. On the other hand, in the saturation zone, where the adsorption maximum, q_{max}, is reached, calorimetric measurements showed that ΔH is equally endothermic, suggesting the need that the overall variation in entropy should be positive to

ensure that the entropic component, $-T \cdot \Delta S$, is negative and, in absolute value, greater than the enthalpic component ($\Delta H > 0$). In addition, the free energy of adsorption will depend on the pH of the solution since this defines the surface charge density of the enzyme and the nanoparticle, affecting the number of electrostatic interactions that can be established. In turn, the ionic strength of the medium will have a monotonically and unfavorable effect on the purely electrostatic processes. This will be attributed to the shielding of the electrostatic interactions that occur because of the transport of ions from the solution to the enzyme–surface interface and the establishment of the electrical double layer that arises because of charge redistribution.

Table 1. Fitting parameters of the adsorption isotherm of protein/enzymes adsorbed on Fe_3O_4.

Enzyme/Protein	Support	Isotherm Adjust	K_d (μM)	q_{max} (mg g^{-1})	Ref.
Cellulase		Langmuir		$\dfrac{370}{430}$	[92]
Bovine hemoglobin (BHb) Bovine serum albumin (BSA) Lysozyme (Lyz)	Cu^{2+}-EDTA-Fe_3O_4	Langmuir and Freundlich (better fit results with Langmuir model)	-	1277 311 192	[114]
Bovine hemoglobin (BHb) β-Lactoglobulin (β-Lac) Lysozyme (Lyz) α-Lactalbumin (α-Lac) Bovine serum albumin (BSA) Fetuin	Fe_3O_4@ytterbium silicate microspheres	Langmuir and Freundlich (better fit results with Langmuir model)	-	304.4 ~75 ~60 ~50 ~45 ~32	[115]
Lysozyme	Fe_3O_4 [C4MIM]-Fe_3O_4 [C6MIM]-Fe_3O_4 [C8MIM]-Fe_3O_4	Langmuir and Freundlich (better fit results with Langmuir model)	17.9 3.8 3.0 6.0	370.4 400.0 500.0 526.3	[116]
Mms6 (magnetosome membrane specific protein)	SP35 (spherical magnetite nanoparticle)	Langmuir	9.52	11.1	[117]
Lipase (BSA as standard protein)	Bare Fe_3O_4	Langmuir	-	19.3	[118]
Bovine serum albumin (BSA)	Nickel ferrite nanoparticles	Langmuir	-	916	[119]
Lysozyme Ovalbumin Conalbumin	Poly(sodium 4-styrenesulfonte) PSS@Fe_3O_4	Langmuir and Freundlich (better fit results with Langmuir model)	-	476.2 4.5 1.8	[120]
α-amylase	Cellulose(28 wt.%)@Fe_3O_4	Langmuir	-	18.2	[121]
Ureasa	Fe_3O_4/SiO_2/APTES Fe_3O_4/SiO_2/APTES/MTES Fe_3O_4/SiO_2/APTES/PTES Fe_3O_4/SiO_2/TMPED	Langmuir	0.12 0.063 0.08 5.0	~300 ~450 ~1000 ~500	[122]

BSA: Bovine Serum Albumin; EDTA: Ethylenediaminetetraacetic acid; C_4MIM, C_6MIM, C_8MIM: ionic liquids, butyl, hexyl or octyl-methylimidazolium; APTES: aminopropyltriethoxysilane; MTES: methyltriethoxysilane; PTES: *n*-propyltriethoxysilane; TMPED: *N*-[3-trimethoxysilylpropyl]ethylendiamine.

As for the thermodynamic parameters that govern the adsorption process, such as ΔH, ΔS, ΔG and K_d, the literature that collects this characterization on magnetite nanoparticles is relatively scarce. Table 3 shows some works reporting these parameters. Of the four shown, two characterize it by calorimetry, ITC (isothermal titration calorimetry), and the other two by performing adsorption isotherm at different temperatures. As for ITC, it is a technique that has proved to be very useful to study the interaction of biomolecules with nanoparticles [123], although it may not be easy to characterize this process, since in most cases, more than one process can be used, as mentioned by Zhao T. et al. [124] in their

characterization of the adsorption of lysozyme and BSA on coated magnetite nanoparticles. As for BSA, they were not able to characterize the adsorption well, with enthalpy values close to 0. For lysozyme, only one of the synthesized nanoparticles, PAA-Fe$_3$O$_4$, could determine the thermodynamic parameters, where the two processes mentioned above occur. In the first stage, the binding process takes place followed by a second step of aggregation and precipitation. The first process is dominated by the entropic contribution since it has a low enthalpy. The second is dominated by a large enthalpy change. Leitner N.S. et al. [125] also used this technique for the characterization of the adsorption of HSA and Human IgG on coated magnetite nanoparticles. They could establish a qualitative discussion of the thermodynamic data obtained because they used a very low concentration in the titration. The enthalpy changes were attributed to changes in the hydrogen bonding and van der Waals interactions, while the entropic changes were mainly associated with hydrophobic interactions and/or conformational changes. From the data collected in Table 3, the HSA binding process showed a highly exothermic enthalpy, so the binding must be guided by van der Waals interactions. The small and negative value of the entropic change is related to a more ordered system after the binding occurs.

Table 2. Enthalpy and entropy contributions to the adsorption process.

Enthalpy Contributions	
Electrostatic interaction	ΔH negligible vs. $-T\Delta S$
Hydrophobic interaction	$\Delta H > 0$ (unfavorable to a.p.)
Entropy Contributions	
Decrease in the translational, rotational and vibrational entropy	$\Delta S_{config} < 0$ (unfavorable to a.p.)
Reduction in conformational stability of the adsorbed enzyme	$\Delta S_{conform} > 0$ (favorable to a.p.)
Release of a large number of water molecules solvating both the nanoparticle surface and the residues exposed to the solvent by the enzyme	$\Delta S_{hydrat} > 0$ (most favorable factor to a.p.)

a.p.: adsorption process.

Table 3. Thermodynamic parameters of adsorption enzymes on surface.

Enzyme/Protein	Support	Method of Determination	K_d (µM)	ΔH (kJ mol^{-1})	ΔS (kJ K^{-1} mol^{-1})	ΔG (kJ mol^{-1})	N	Ref.
Lysozyme	Fe$_3$O$_4$ [C4MIM]-Fe$_3$O$_4$ [C6MIM]-Fe$_3$O$_4$ [C8MIM]-Fe$_3$O$_4$	From adsorption isotherm at different temperatures	17.9 3.8 3.0 6.0	−12.3 31.0 11.5 16.6	−0.036 0.129 0.053 0.071	1.72 −7.38 −4.26 −4.60	-	[116]
BSA Lysozyme	DEAPA-Fe$_3$O$_4$ PAA-Fe$_3$O$_4$ DEAPA-Fe$_3$O$_4$ PAA-Fe$_3$O$_4$	ITC	- - - 1p: 0.14 2p: 29.4	~0 ~2 kcal mol^{-1} ~0 1p: −2.2 2p: −27.2	- - - 1p: 0.12 2p: −0.004	- - - 1p: −39.2 2p: −25.9	- - - 14.6 69.5	[124]
HSA Human IgG	5_Fe$_3$O$_4$-PAOZ 8_Fe$_3$O$_4$-PAOZ 5_Fe$_3$O$_4$-PAOZ 8_Fe$_3$O$_4$-PAOZ	ITC	3.1 34 1.6 0.4	−320 −240 −340 −110	−1.0 −0.7 −1.0 −0.26	−31.6 −25.6 −34.1 −36.5	2.2 7.0 1.1 0.9	[125]
Trypsin	PVPr-co-P4VP/Fe$_3$O$_4$ hydrogel	From adsorption isotherm at different temperatures	316.4 (a)	20.4	0.116	−14.26	-	[126]

N: binding stoichiometry; PAA: poly(acrylic acid); BSA: Bovine Serum Albumin; DEAPA: (PAA)-co-3-(diethylamino)-propylamine; ITC: Isothermal Titration Calorimetry; 1p: first process, 2p: second process; HSA: Human Serum Albumin; IgG: immoglobulin G; PAOZ: poly(2-alkyl-2-oxazoline); PVPr-co-P4VP: copolymer of polyl-N-vinylpyrrolidone and poly-4-vinylpyridine; (a): dimensionless; [C4MIM], [C6MIM] y [C8MIM]: ionic liquids.

3.3. Kinetic and Thermodynamic Parameters of Immobilized Enzymes

Once the enzyme is immobilized, thermodynamic and kinetic parameters can be characterized to determine the thermal stability of the enzyme. In the case of kinetic parameters, we can determine the Michaelis–Menten constants (K_m) and the rate of the reaction catalyzed by the enzyme from the maximum velocity (V_{max}). V_{max} is a characteristic feature of an enzyme at a specific substrate concentration. K_m is an inverse measure of the affinity for the substrate and predicts the relationship between the rate of product formation from the substrate concentration at the conditions under which the reaction is occurring. On the other hand, in terms of thermodynamic parameters, E_d, ΔH, ΔS and ΔG are related to the stability and functionability of the enzyme at the conditions under which the reaction is carried out. On the one hand, E_d, the deactivation energy, is the minimum amount of energy required to trigger the denaturation process of the enzyme, and thus inactivate it. The enthalpy, ΔH, is the amount of energy required to produce the denaturation of the enzyme. ΔG is the amount of usable energy that arises during the deactivation process, and also indicates the spontaneity of the thermal denaturation process caused by conformational changes and the breaking of various bonds. Entropy, ΔS, is the energy per degree required to produce the conformational change in the enzyme from the native state to the denatured state (related to the local disorder between the two states) [127,128].

In almost all the cases reported in this review, there is an increase in the thermal stability of the immobilized enzyme with respect to the free enzyme (Table 4). Such immobilization results in a reduction in the efficiency and affinity of the enzyme for the substrate after immobilization. Bindu V.U. et al. [129] immobilized α-amylase on chitosan-coated magnetite nanoparticles, on which they adsorbed directly or immobilized by covalent bonding using glutaraldehyde, glyoxal or epichorohydrin. With immobilization, stability is improved by 60–80% over the free enzyme; this is more noticeable when immobilization is covalent versus adsorption, probably due to the protection to conformational changes through such bonds on the surface. Comparing the ΔG in all cases, there is an increase in this value, so that the stability improves after immobilization. As for the kinetic parameters, they obtain that K_m is higher, so the affinity on the substrate decreases, possibly due to structural changes in the enzyme. Because of this, V_{max} is also lower for the immobilized enzyme than for the free enzyme.

Wong. W.K.L. et al. [130] covalently immobilized *Candida rugosa* lipase on silica-coated magnetite nanoparticles. These authors also observed an improvement in the stability of the immobilized enzyme with respect to the free enzyme (E_d free: 93.3, E_d immobilized: 112.9). This is corroborated due to the increase in Gibbs free energy, making the denaturation process less spontaneous. Although Vmax decreased for the immobilized enzyme, in this case, they found a 12-fold increase in the affinity of the enzyme for the substrate. They attributed this to surface activation with glutaraldehyde which increased the biocompatibility of the surface to form covalent bonds with the enzyme.

Table 4. Thermodynamic and kinetic parameters of free and immobilized enzymes.

Enzyme/ Protein	Support	Method Immo.	Ed (kJ mol⁻¹)		ΔH (kJ mol⁻¹)		ΔS (kJ K⁻¹ mol⁻¹)		ΔG (kJ mol⁻¹)		Km (mg/mL)		Vmax (µmol ml⁻¹ min⁻¹)		Reference
			f	i	f	i	f	i	f	i	f	i	f	i	
Catalase	Fe₃O₄/SiO₂ _____ mSiO₂@Fe₃O₄/SiO₂	Covalent	-	-	-	-	-	-	-	-	15.3 (mM)	16.6 / 21.2	4.02	3.47 / 2.36	[104]
α-amylase	CSM-Fe₃O₄ CSM-GLY-Fe₃O₄ CSM-GLA-Fe₃O₄ CSM-CSM-Fe₃O₄	Adsorption Covalent Covalent Covalent	15.3	18.8 35.4 28.3 23.6	12.7	16.2 32.8 25.7 21.0	−0.28	−0.28 −0.24 −0.26 −0.27	101.7	104.2 106.8 106.4 104.8	0.45	1.03 0.53 0.57 0.65	34.48 *	15.4 * 25.0 * 19.6 * 16.4 *	[129]
Candida rugosa lipase (CRL)	AP-SiO₂-Fe₃O₄	Covalent	93.3	112.9	87.7	110.3	233.7	293.2	14.6	17.0	6000	583	3330	833.3	[130]
Inulinase	GSH-Au-Fe₃O₄	Covalent	-	-	-	-	-	-	-	-	5.4	6.8	3.55	3.03	[131]
α-amylase	GO-Fe₃O₄	Covalent	85.4	79.0	74.2	79.1	−0.17	−0.14	114.3	106.2	0.6	0.9	450	333.3	[132]
β-Glucosidase	Bare Fe₃O₄	Covalent	-	-	-	-	-	-	-	-	3.5 (mM)	4.3 (mM)	0.72	0.89	[133]
Candida rugosa lipase (CRL)	A-SiO₂-Fe₃O₄	Covalent	113.9 (ag.)	128.5	111.2 (ag.)	122.8	0.29 (ag.)	0.32	16.8 (ag.)	18.3	13.8 (mM)	18.0 (mM)	0.30	0.28	[134]
Laccase	Fe₃O₄-SiO₂-AP	Covalent	-	-	-	-	-	-	-	-	0.0015 (mM)	0.0062 (mM)	0.32	0.062	[135]
α-amylase	ZnO-Fe₃O₄	Adsorption	18.9	21.6	15.5	18.8	−0.28	−0.28	108.3	110.9	0.61	0.65	18.7 mg ml⁻¹ min⁻¹	18.2 mg ml⁻¹ min⁻¹	[136]
Candida rugosa lipase (CRL)	SiO₂/Fe₃O₄/GO	Covalent	27.6	32.3	25.0	29.7	0.035	0.048	13.8	14.5	-	-	-	-	[137]

f: free; i: immobilized; Ed: activation energy of denaturation; CSM: Chitosan; GLY: glyoxal; GLA: glutaraldehyde; GO: Graphene oxide; AP or A: 3-aminoporpyltriehoxysilane; ag.: aggregated CRL; *: µmol mg⁻¹ min⁻¹; mSiO₂: mesoporous silica.

4. Enzyme–Magnetite Nanohybrids for Catalytic Biotechnology

The use of free enzymes in biomedical, industrial and analytical processes may pose several drawbacks: (i) short half-lives and an unstable structure that could denature and lose their native conformation, and in turn their activity, if they are not in optimal conditions; (ii) difficulties in terms of recovery and reuse for subsequent processes. For this reason, there has recently been a growing interest in the development of carriers and immobilization strategies. Thus, by applying an external magnetic field, we could recover the enzyme from the reaction, improve the stability, reuse the enzyme in continuous operational cycles and reduce the limitations in the diffusion of substrates and products, as well as increase the functional surface area and, thus, the loading capacity [6]. Herein, we include a selection of catalytic applications properly summarized in Table 5 but the interested readers can find other excellent reviews in the literature [5,25–28,49,138–140]. For instance, Mehrasbi et al. [141] covalently attached the lipase enzyme to magnetic nanoparticles (MNPs) for biodiesel synthesis. It was observed that the immobilized enzyme preserved 97% of its activity with respect to the free enzyme, maintaining 100% of the initial activity after 6 reaction cycles. A positive aspect of immobilizing enzymes that has been named before is the reusability and recovery of enzymes to avoid economic losses and, in this case, it was possible. In addition, in the industrial sector, Kharazmi et al. [142] covalently attached pectinase enzyme to PEG-functionalized magnetic nanoparticles, employing, subsequently, cyanuric chloride. In this process, they were able to improve enzyme activity and stability and easily recover the enzyme for further use. Other systems have been developed for biomedical applications using nanobiocatalysis. Kempe et al. [143] designed MNPs to treat thrombosis in coronary arteries. For this purpose, the MNPs were coated with silica (silanol groups) in the presence of triethylene glycol (TREG) and/or PEG. Subsequently, this coating was activated by NHS/EDC or tresyl chloride for the covalent binding of tissue plasminogen activator (tPA) enzyme (Figure 3). Marques da Silva et al. [144] immobilized the enzyme fibronolytic protease (FP) to MNPs. These are coated with polyaniline and subsequently activated with glutaraldehyde to create a covalent bond between the enzyme and the MNPs. This procedure allowed for the retention of the enzyme at 52% and the activity was maintained at 60% at a temperature between 40 °C to 60 °C and a pH of 7 to 10, compared to the free enzyme. It was observed that the enzyme maintained thrombolytic activity and showed total degradation of the human fibrinogen γ-chain, and could, therefore, be used for the treatment of cardiovascular diseases.

Table 5. Examples of enzymes immobilized on coated $F_{e3}O_4$ and biocatalytic applications.

Enzyme	Coating Reagent	Fe_3O_4 Preparation Method	Immobilization Method	Application Field	Specific Applications	Ref.
Lipase A	Chitosan	Co-precipitation	Covalent (Glutaraldehyde)	Industry	Biolubricants production	[3]
Lipase A Lipase B	APTES	Co-precipitation	Covalent (Glutaraldehyde)	Industry	Ethyl butyrate production	[20]
Catalase	Silica (TMOS, APTES)	Solvothermal	Covalent (Glutaraldehyde)	Scientific purpose	Enzyme shielding	[104]
Lipase	Silica magnetic nanoparticles on (3-glycidoxypropyl) trimethoxylsilane (GPTMS)	Co-precipitation	Covalently (Epoxy groups/nucleophilic groups on the surface of enzyme)	Industry	Biodiesel production	[141]
Pectinase	Polyethilene glycole (PEG)	Co-precipitation	Covalent (trichlorotriazine Cyanuric chloride)	Industry	Fruit juice clarification	[142]
Tissue plasminogen activator (tPA)	Silica (TEOS, PEG, TREG)	Oxidation-precipitation	Covalent (NHSS-EDC and tresyl chloride)	Medicine	Treatment of thrombosis in coronary arteries	[143]

Table 5. *Cont.*

Enzyme	Coating Reagent	Fe$_3$O$_4$ Preparation Method	Immobilization Method	Application Field	Specific Applications	Ref.
Fibrinolytic protease (FP)	Polyaniline	Precipitation	Covalent (Glutaraldehyde)	Medicine	Treatment of cardiovascular diseases (degradation of the γ chain of human fibrinogen)	[144]
Glucose oxidase (GOx)	-	Co-precipitation	Adsorption	Industry	Removal of acid yellow 12	[145]
Glucose oxidase (GOx)	Magnetic nanoparticles (EM1-100/40)	Purchased from Merck Co.	Covalent	Scientific purpose	Study of enzyme inactivation	[146]
Lipase	Polymer-coating (Gum Arabic)	Co-precipitation	Covalent (Glutaraldehyde)	Industry	Biocatalyst a flavor ester, production	[147]
Lipase	AGMNP-Co^{2+}	Co-precipitation	Metal chelate affinity	Industry	Biodiesel production	[148]
Lipase	Polyaniline (Pani)	Co-precipitation	Adsorption	Scientific purpose	Enzyme adsorption	[149]
β-fructofuranosidase	Chitosan	Co-precipitation	Adsorption	Industry	Produce fructooligosaccharides (growth of desirable gut microflora)	[150]
Tripsin	Gallic acid (GA)	Co-precipitation	Adsorption	Industry	Hydrolysis of bovine milk	[151]
L-Asparaginase	Amine-functionalized silane modifier, APTES	Co-precipitation	Covalent	Industry	Reduce acrylamide content in the food system (carcinogen and neurotoxin)	[152]
β-agarase	Tannic acid (TA)	Co-precipitation	Adsorption	Industry	Bioactive neogaro-oligosaccharide (varying antioxidant activities)	[153]
D-allulose-3-epimerase	ZIF67 (MOF)	Solvothermal	Encapsulation into ZIF67 (Chemical bonds Co^{2+})	Industry	Preparation of D-allulose (rare low-calorie sugar)	[154]
Horseradish peroxidase (HRP)	Polymethil methacrylate (PMMA)	Purchased from Sigma-Aldrich	Encapsulation	Industry	Removal of wastewater aromatic pollutants	[155]
Ene-reductase	Non-functionalized MNP (After add (HR)$_4$tag)	Co-precipitation	Adsorption	Scientific purpose	Study enzyme immobilization	[156]
Sortase A	Peptide	Co-precipitation	Covalent	Scientific purpose	Produce and bioquemically characterize immobilized proteins (single-molecule FRET)	[157]
β-D-galactosidase (lactase)	Fe$_3$O$_4$–chitosan (Fe$_3$O$_4$–CS)	Co-precipitation	Covalent (Glutaraldehyde)	Industry	Galactooligosaccharides (GOS) production	[158]
Tyrosinase	Magnetic beads poly(GMA–MMA)	Co-precipitation	Covalent ((Glutaraldehyde)	Industry	L-Dopa (1-3,4-dihydroxy phenylalanine)	[159]

AGMNP: 5-Aminoisophthalic acid (5-AIPA) (A), 3-Glycidoxypropyltrimethoxysilane (GOPTS) (G), MNP (Magnetic Nanoparticles); ZIF67 (MOF): Zeolitic imidazolate frameworks (metal–organic frameworks); TMOS: Tetramethyl orthosilicate, APTES: aminopropyltriethoxysilane; PEG: Polyethylene glycol; TREG: tetraethylene glycol; (HR)4tag: (His-Arg)$_4$ peptide-tag;; EM1-100/40: 57 μequiv. of COOH/g, containing 54% ferrite; MMA: methyl methacrylate.
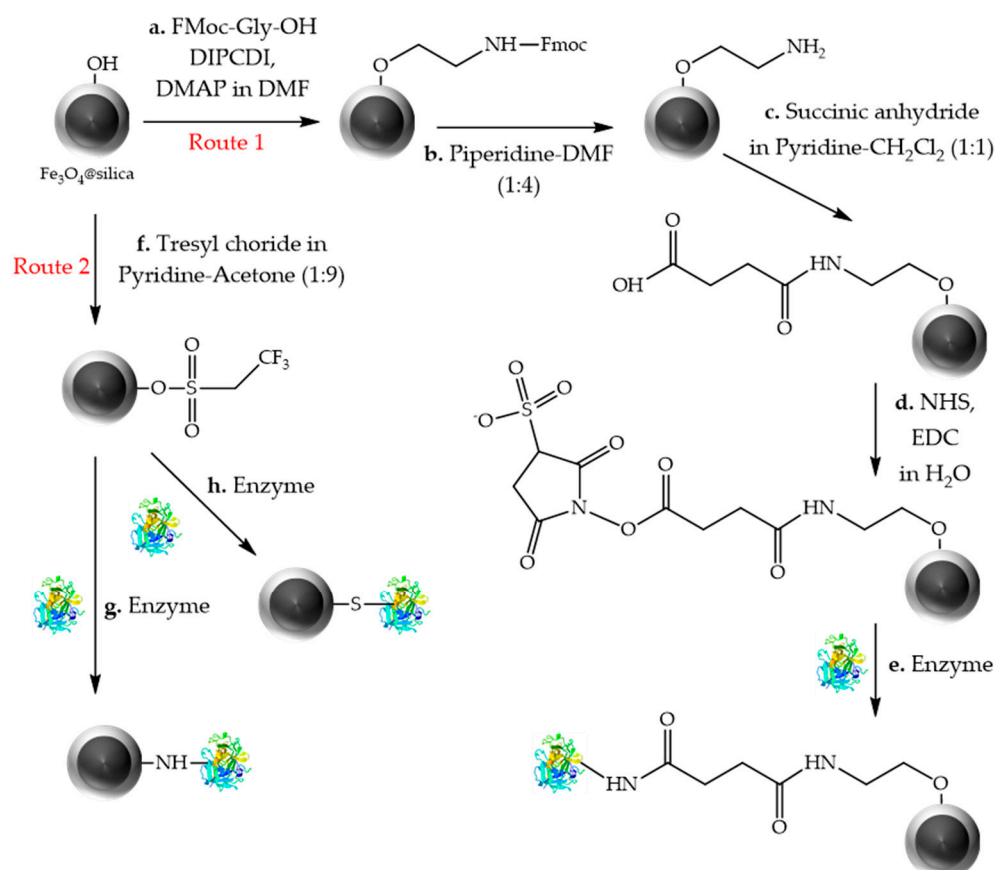
Figure 3. Immobilization of tPA on Fe₃O₄@silica. Route 1. Activation of surface-coated NPs with NHS-EDC. (**a**) Coupling of Fmoc-Gly-OH to silica surface NPs. (**b**) Removal of Fmoc group. (**c**) Succinylation of the free amino groups. (**d**) Esterification of NPs through activation by addition of NHS/EDC. (**e**) enzyme immobilization. Route 2. Tresyl chloride activation of surface-coated NPs (**f**–**h**) Enzyme immobilization through amino or thiol groups. Adapted from [143].

Aber et al. [145] designed a system for acid yellow 12 decolorization by a bio-Fenton process in which they immobilized the GOx enzyme on magnetic nanoparticles by means of an adsorption process. In their study, they found that after 15 washing cycles, the immobilized enzyme lost only 6.5% of its initial activity. Interestingly, Betancor et al. [146] proposed the use of dextran aldehyde to potentially minimize the deactivation of GOx immobilized onto MNPs under challenging operational conditions. Cui et al. [104] proposed a reusable and stable nanobiocatalyst by means of an enzyme-shielding strategy. For this purpose, they immobilized the catalase enzyme on magnetite nanoparticles functionalized with APTES, subsequently protecting it with a silica layer. They showed that the protection enabled the enzyme to maintain 70% of its activity after 9 cycles, while the unprotected enzyme retained only 20%.

5. Enzyme–Magnetite Nanohybrids for Cancer Therapy

MNPs have emerged as a promising tool for cancer therapy due to their unique physical and chemical properties. They can be used for various purposes, such as targeted drug delivery, hyperthermia and magnetic resonance imaging (MRI). Magnetic nanoparticles can be used as contrast agents for MRI to help visualize tumors. They can serve as contrast agents for MRI, generating local magnetic fields that can alter the relaxation times of the protons in water. This alteration can lead to changes in the signal intensity and help to distinguish between normal and abnormal tissues [160,161]. MNPs can also be exploited as a heat source for optical and magnetic hyperthermia since they can be heated up by an alternating magnetic field (AMF) applied externally (Figure 4). When magnetic nanoparti-

cles are exposed to an AMF, the magnetic moments of the nanoparticles oscillate rapidly, causing frictional heating, which can lead to the generation of heat [162]. Additionally, several studies highlight MNPs as an excellent platform for drug delivery [163]. Due to their biocompatibility and superparamagnetic properties, conjugated drug-MNPs have been developed as carriers [164].
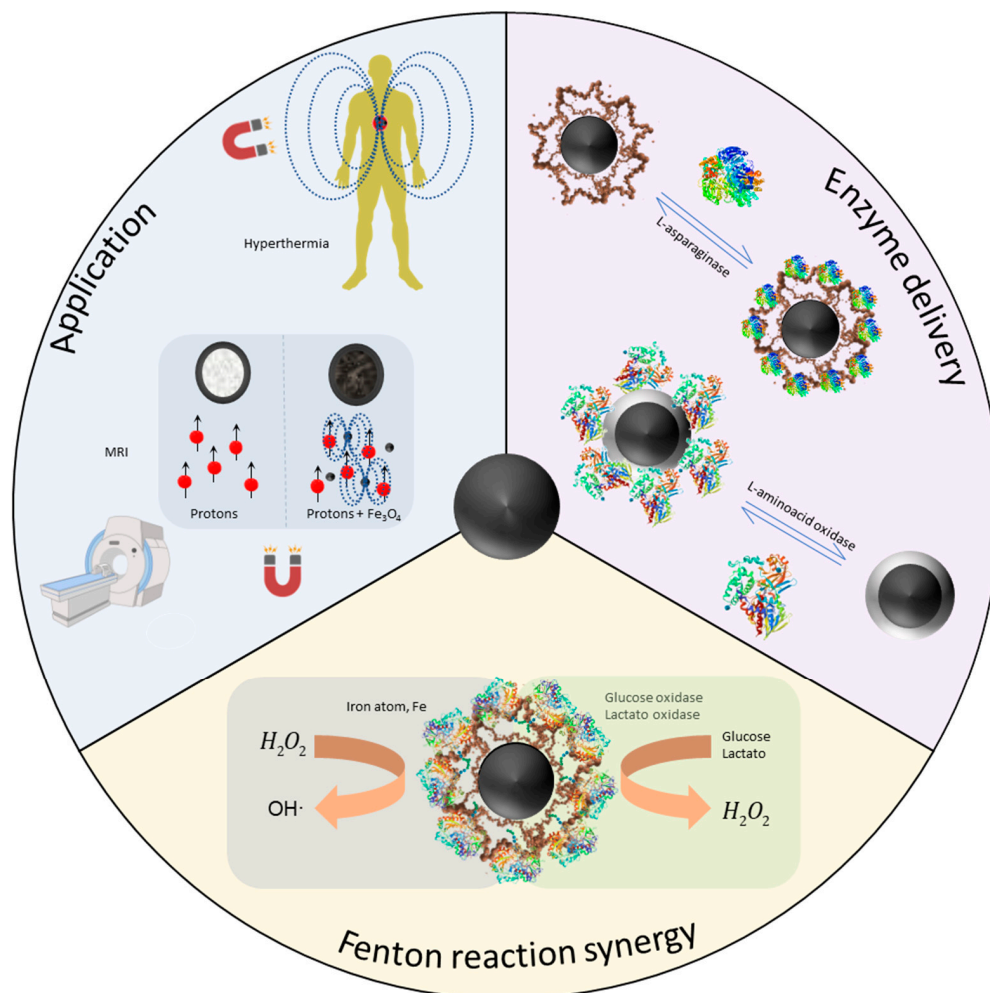

Figure 4. Different uses of functionalized enzyme–magnetite nanocomposites in cancer therapy. (Some images have been created in BioRender.com (accessed on 29 May 2023)).

However, in the last few years, MNPs have been systematically applied in CDT. This therapy utilizes a Fenton or Fenton-like reaction to generate highly cytotoxic hydroxyl radicals ($\bullet$OH) from H_2O_2 to promote oxidative stress and induce cancer cell apoptosis [165]. The tumor microenvironment (TME) plays a crucial role in cancer progression and response to CDT. The overexpression of endogenous H_2O_2 in tumors (1 mM) and the low pH lead MNPs to efficiently tackle tumor-specific sites via CDT. This strategy has been widely exploited in combination with other ROS-assisted therapies such as PDT [166–168], EDT [169] or PTT [170] in order to improve the ROS killing ability. Alternatively, Wang and co-workers developed a novel nanocatalyst platform with a longer half-life time ROS generation. Most cytotoxic hydroxyl radicals have a short half-life time of ~1 µs. These ROS half-life times may affect cell damage especially for primary organelles delivery. They used Fe_3O_4–Schwertmannite nanocomposites (Fe_3O_4-Sch). MNPs perform a Fenton reaction and the Schwertmannite shell converts the $\bullet$OH into sulfate radicals with a longer half-life time (30 µs), overwhelming tumor inhibition efficacy. Nevertheless, the success of CDT depends on the concentration of H_2O_2 present in the TME. Thus, endogenous H_2O_2 can

act as a bottleneck to perform CDT. Various strategies have been developed to increase the concentration of H_2O_2 in the TME by adding exogenous H_2O_2. Enzymes that generate H_2O_2 can play an important role in the catalytic antitumor therapy of MNPs. Enzymes such as glucose oxidase (GOx), D/L-amino acid oxidase (D/LAAO) or lactate oxidase (LOx) can react with different substrates such as glucose, D/L-amino acids or lactate, respectively, and, in situ, form H_2O_2 and enhance CDT [171].

GOx has attracted significant attention and has been successfully applied in cancer research [172]. This enzyme leads to the consumption of glucose, which provides an alternative strategy for cancer-starvation therapy. Furthermore, the O_2 depletion leads to increased tumor hypoxia and gluconic acid enhances tumor acidity (Figure 4). Thus, GOx/MNPs nanohybrids have been considered as promising candidates as antitumor agents [173]. Of all the articles reviewed, a very low percentage of authors (10–15%) apply the use of enzyme immobilization on magnetite nanoparticles for cancer therapy (Table 6). Some authors combined the use of magnetite nanoparticles with the use of enzymes for cancer therapy, although there is no direct immobilization of the enzyme on the nanoparticle. For example, Wu J. et al. [174] designed hybrid motors conjugated with glucose oxidase (GOx) and magnetite nanoparticles. Gox, in addition to serving as a motor for self-propulsion by degrading glucose, hinders cellular metabolism by consuming glucose. Magnetic nanoparticles serve as a magnetic motor, increasing the kinetic power and achieving a higher directionality toward the tumor. Qin X. et al. [175] designed hybrid nanogels loaded in the innermost part with magnetite nanoparticles, while in the most superficial part, they encapsulated lactate oxidase and catalase enzymes. With this system, they were able to raise ROS levels significantly, thereby causing cell death and, thus, inhibiting tumor growth.

Table 6. Examples of enzymes immobilized on coated Fe_3O_4 for cancer therapy applications.

Enzyme	Coating Reagent	Fe$_3$O$_4$ Preparation Method	Immobilization Method	Specific Applications	Ref.
Glucose oxidase (GOx)	Silica (TEOS, EPTES)	Co-precipitation	Covalent (Glutaraldehyde)	Cytotoxic study for biomedical applications	[176]
Choline-binding domain of N-acetylmuramoyl-L-alanine amidase–D-amino acid oxidase (CLytA-DAAO)	Diethilaminoethanol (DEAE)	Purchased from Chemicell GmbH (Berlin, Germany)	Adsorption (between CLytA domain and DEAE)	Anticancer therapy for pancreatic and colorectal carcinoma and glioblastoma	[177]
LDHA (isoenzyme of Lactate Dehidrogenase, LDH)	Amino groups (APTES)	Co-precipitation	Covalent (Glutaraldehyde)	Cancer treatment (identification of LDH inhibitors)	[178]
β-Glucosidase	Polyethylene glycol, PEG (by hydroxy-succinimide chemistry)	Purchased from Chemicell GmbH (Berlin, Germany)	Covalent (Glutaraldehyde)	Enzyme/Prodrug therapy in cancer	[179]
L-Asparaginase	Poly(2-vinyl-4,4-dimethylazlactone	Co-precipitation	Covalent	Construct an efficient enzyme reactor (potential application in leukemia treatment)	[180]
L-Asparaginase	Poly(HEMA-GMA)	Purchased from Sigma-Aldrich (St. Louis, MO, USA)	Covalent	Lymphoblastic leukemia (Remove L-Asparagine, an essential factor of protein synthesis)	[181]
Glucose oxidase (GOx)	Fe$_3$O$_4$@PDA	Purchased from Sigma-Aldrich St. Louis, MO, USA)	Adsorption	Cancer treatment	[182]

TEOS: Tetraethyl orthosilicate; EPTES: N-(β-ethylenamine)-γ-propylamine triethoxylsilan; APTES: aminopropyl-triethoxysilane; Poly(HEMA-GMA): 2-hydroxyethyl methacrylate (HEMA), glycidyl methacrylate (GMA); PDA: polydopamine; DDAO: D-amino acid oxidase.

Ashtari et al. [176] immobilized the GOx enzyme onto silica-coated magnetite nanoparticles, whose surface had been previously functionalized with amino groups. They concluded that the proposed system had a potential application in biomedicine since the covalent binding of the enzyme increases its conformational stability compared to the free enzyme. In addition, it maintained its activity after storage for 45 days, compared to 15 days for the free enzyme. Finally, the proposed system was reused for 12 cycles where the GOx kept its activity at 90%, and even for 20 cycles, although the activity dropped to 50%.

Zhou et al. [179] conjugated a β-glucosidase enzyme to aminated magnetite nanoparticles using glutaraldehyde and the subsequent use of PEG (Figure 5A). They found the Michaelis constant to evaluate the activity of β-glucosidase on MNPs, where they observed that 73% and 65% of the enzyme activity was maintained for β-Glu-MNP and PEG-β-Glu-MNP, respectively, compared to the free enzyme. Another enzyme employed in cancer treatment was L-asparaginase since tumor cells, especially lymphatic tumor cells, require a large amount of asparagine to maintain rapid proliferation. Mu et al. [180] employed MNPs functionalized with the polymer poly(2-vinyl-4,4-dimethylazlactone) for the subsequent covalent binding of the enzyme (Figure 5B). They observed that the enzyme maintained more than 96% of its activity after 10 consecutive uses and more than 73% of the activity after 10 weeks, concluding that it could be a good treatment in leukemia. Orhan et al. [181] also immobilized the enzyme L-asparaginase to magnetite nanoparticles as a treatment for leukemia. In this case, the MNPs were functionalized with Poly(HEMA-GMA) (Figure 5C). Immobilization in most cases, as we have seen in the previous examples, stabilized the enzyme and prolonged the lifetime of the enzyme. In this case, it also occurs, observing an almost total loss of free enzyme activity at 10 h, while 50% of the activity was preserved in the case of the enzyme supported on the MNPs.

Zhang et al. [182] developed polydopamine (PDA)-coated magnetite nanoparticles on which they covalently bonded GOx. The PDA coating serves as photothermal transfer materials converting near infrared (NIR) radiation into heat. With GOx, by consuming glucose and generating H_2O_2, the magnetite nanoparticles can be converted into $^\bullet OH$ radicals, inducing apoptosis of cancer cells.

Zhang et al. [183] established a novel strategy to develop a precise regulation of enzyme–nanozyme cascade reaction kinetics by remote magnetic stimulation. GOx was immobilized onto MNPs functionalized with poly(ethylene glycol) (PEG) of different molecular weights. They found an optimum linking distance of 1 nm which exhibited a superior kinetic match between GOx and the MNPs (over 400-fold higher) for cascade activity under AMF exposure. GOx was covalently immobilized onto the Fe_3O_4 NR using the EDC/NHS method.

Analogously, other relevant studies highlight the use of D/LAAO as an exogenous H_2O_2 supplier. Fuentes-Baile et al. [177] bound the enzyme D-amino acid oxidase (DAAO) that catalyzes the oxidation of D-amino acids generating H_2O_2. This enzyme bound to the N-acetylmuramoyl-L-alanine amidase (CLytA) domain proved to be cytotoxic in several glioblastoma cell lines and pancreatic and colorectal carcinomas [184]. The MNPs used were coated with Diethilaminoethanol (DEAE) for subsequent adsorption between the CLytA domain and DEAE. They observed that immobilization increased the stability of the enzyme at 37 °C, prolonging its catalytic activity over time, and that the cytotoxic effect was due to prolonged ROS generation and suggested that it could be a good system as an antitumor therapy in patients with glioblastoma, pancreatic and colorectal carcinomas.
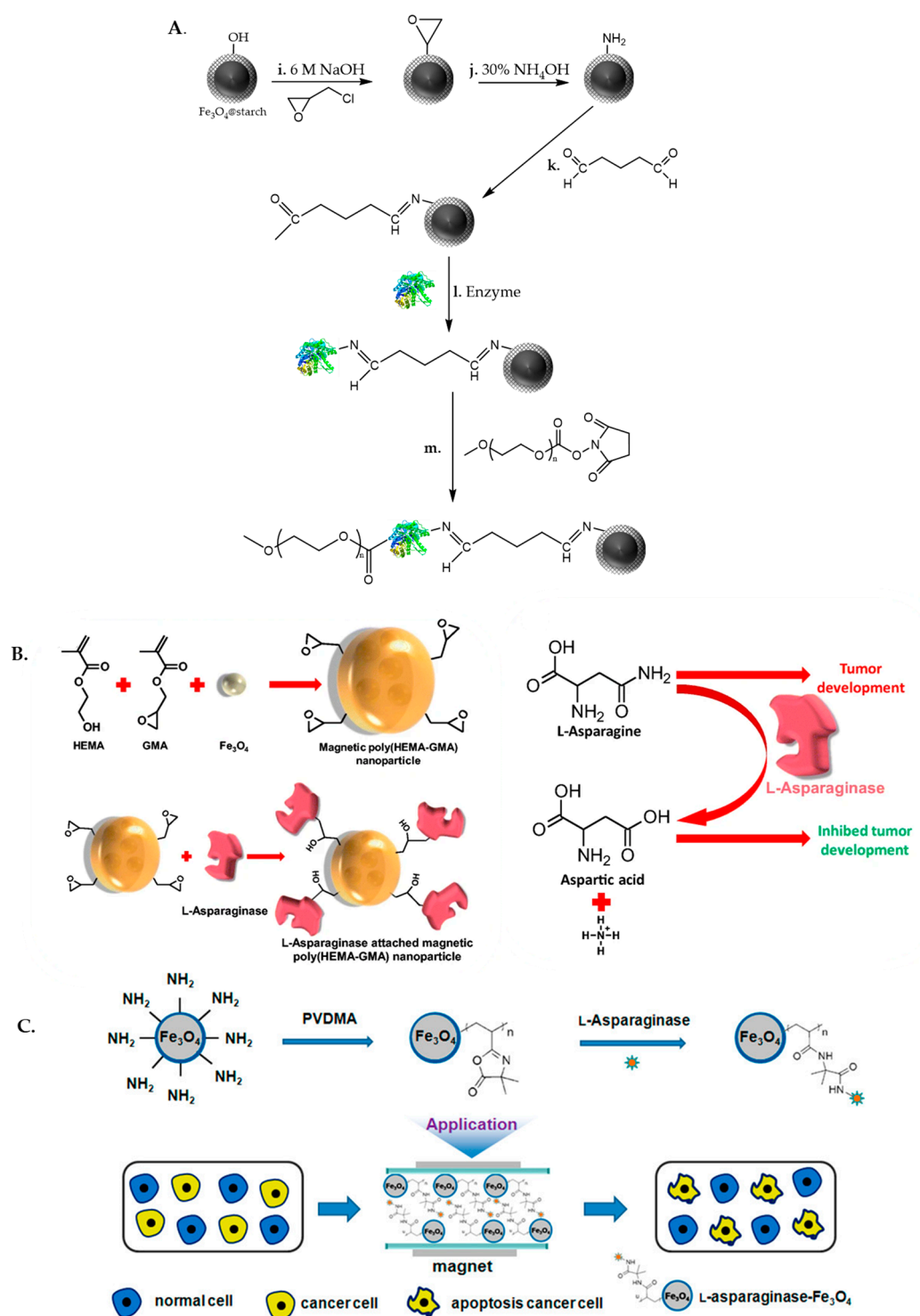
Figure 5. (**A**). Immobilization of β-glucosidase on Fe$_3$O$_4$@starch. i., j. Cross-linked and aminated by modification of the surface using epichlorohydrin and concentrated ammonium hydroxide. k., l. Enzyme immobilization by glutaraldehyde method. m. Modification of enzyme with PEG using NHS (SC-NHS-PEG). In (**B**,**C**). L-Asparaginase immobilization onto two different systems. (**B**). Schematic presentation of the synthesis of magnetic poly(HEMA-GMA) nanoparticles and mechanism of action of L-asparaginase in tumor cells. (**C**). Schematic illustration of L-Asparaginase immobilization onto PVDMA-Modified Magnetic Nanoparticles and simulation of extracorporeal shunt system using the enzyme reactor. Adapted [179–181].

In the last few years, LOx has been considered an alternative as an exogenous H_2O_2 supplier for MNPs to enhance CDT [185]. The enzymatic process consumes lactate and O_2 increasing hypoxia levels and generates H_2O_2 and pyruvate. Given the high levels of lactate in tumor tissues and its tight correlation with tumor growth, metastasis and recurrence, this enzyme has been considered as an alternative to GOx to perform an enhancement in CDT. Qin et al. [175] tested the reactive oxygen species (ROS) generation and tumor therapy by integrating lactate oxidase (LOx), catalase (CAT) and indocyanine green (photosensitizer) into MNPs. LOx and CAT cascade catalytic metabolic regulation was used to form hydroxyl radical ($\cdot$OH) and singlet oxygen ($^1O_2$) production by using NIR-trigger PDT.

6. Conclusions

The combination of enzymes and MNPs as synergistic nanoassemblies represents an interesting and appealing catalytic alternative for multiple biomedical and biotechnological applications. This review has provided a thorough description of the process of enzyme adsorption onto magnetic nanoparticles and further insights regarding the thermodynamic and kinetic factors governing the stability and reactivity of immobilized enzymes. The fact that the enzyme is supported on magnetic nanoparticles makes it more attractive given their potential role as co-catalysts, theranostic agents and their use for recyclability or active medical treatment under the influence of magnetic fields. Given the numerous investigations already known about the immobilization of enzymes on magnetic nanoparticles (the possibility of use in diagnosis due to the magnetic core monitoring that the therapy is selectively localized), and given the catalytic activity of these enzymes that can alter the metabolism of tumor cells (via Fenton or ferroptosis), we believe that future research should be aimed at finding selective treatments for cancer therapy, although it is necessary to continue research on the possible ways of vehiculization of such systems. The co-immobilization of several enzymes can also be envisioned as an interesting and challenging field of development [29,186]. Likewise, it should be advisable to improve the efficiency of combined therapies that take advantage of both enzymes and MNPs simultaneously. Bioorthogonal catalysis to promote the development of cascade reactions involving Fe species, ROS and enzymes such as LOx or DAAO can also be another area of great interest for tackling the tumor microenvironment. Furthermore, the potential tracking of enzyme–MNPs nanohybrids within the TME should be further explored in order to understand the fate of these platforms after intracellular internalization and fully understand the fate of these structures and their potential influence in the cell metabolism.

References

1. Jin, S.; Wu, C.; Ye, Z.; Ying, Y. Designed Inorganic Nanomaterials for Intrinsic Peroxidase Mimics: A Review. *Sens. Actuators B Chem.* **2019**, *283*, 18–34. [CrossRef]
2. Del Arco, J.; Alcántara, A.R.; Fernández-Lafuente, R.; Fernández-Lucas, J. Magnetic Micro-Macro Biocatalysts Applied to Industrial Bioprocesses. *Bioresour. Technol.* **2021**, *322*, 124547. [CrossRef] [PubMed]
3. Monteiro, R.R.C.; Lima, P.J.M.; Pinheiro, B.B.; Freire, T.M.; Dutra, L.M.U.; Fechine, P.B.A.; Gonçalves, L.R.B.; de Souza, M.C.M.; Dos Santos, J.C.S.; Fernandez-Lafuente, R. Immobilization of Lipase A from Candida Antarctica onto Chitosan-Coated Magnetic Nanoparticles. *Int. J. Mol. Sci.* **2019**, *20*, 4018. [CrossRef] [PubMed]

4. Mateo, C.; Palomo, J.M.; Fernandez-Lorente, G.; Guisan, J.M.; Fernandez-Lafuente, R. Improvement of Enzyme Activity, Stability and Selectivity via Immobilization Techniques. *Enzyme Microb. Technol.* **2007**, *40*, 1451–1463. [CrossRef]

5. Cipolatti, E.P.; Valério, A.; Henriques, R.O.; Moritz, D.E.; Ninow, J.L.; Freire, D.M.G.; Manoel, E.A.; Fernandez-Lafuente, R.; De Oliveira, D. Nanomaterials for Biocatalyst Immobilization—State of the Art and Future Trends. *RSC Adv.* **2016**, *6*, 104675–104692. [CrossRef]

6. Singh, M.; Ishfaq, N.; Salman, S.; Bashir, M.H.; Ashfaq, B. Enzyme Immobilization and Applications of Magnetic Nanoparticles in Smart Enzyme Immobilization. *Sci. Technol.* **2017**, *3*, 387–396.

7. Nisha, S.; Karthick, A.; Gobi, N. A Review on Methods, Application and Properties of Immobilized Enzyme. *Chem. Sci. Rev. Lett.* **2012**, *1*, 148–155.

8. Wu, W.; Pu, Y.; Shi, J. Nanomedicine-Enabled Chemotherapy-Based Synergetic Cancer Treatments. *J. Nanobiotechnol.* **2022**, *20*, 1–21. [CrossRef]

9. Bonet-Aleta, J.; Hueso, J.L.; Sanchez-Uriel, L.; Encinas-Gimenez, M.; Irusta, S.; Martin-Duque, P.; Martinez, G.; Santamaria, J. Synergistic Assembly of Gold and Copper-Iron Oxide Nanocatalysts to Promote the Simultaneous Depletion of Glucose and Glutathione. *Mater. Today Chem.* **2023**, *29*, 101404. [CrossRef]

10. Bonet-Aleta, J.; Calzada-Funes, J.; Hueso, J.L. Manganese Oxide Nano-Platforms in Cancer Therapy: Recent Advances on the Development of Synergistic Strategies Targeting the Tumor Microenvironment. *Appl. Mater. Today* **2022**, *29*, 101628. [CrossRef]

11. Yang, B.; Chen, Y.; Shi, J. Nanocatalytic Medicine. *Adv. Mater.* **2019**, *31*, 1901778. [CrossRef] [PubMed]

12. Garcia-Peiro, J.I.; Bonet-Aleta, J.; Santamaria, J.; Hueso, J.L. Platinum Nanoplatforms: Classic Catalysts Claiming a Prominent Role in Cancer Therapy. *Chem. Soc. Rev.* **2022**, *51*, 7662–7681. [CrossRef] [PubMed]

13. Imam, H.T.; Marr, P.C.; Marr, A.C. Enzyme Entrapment, Biocatalyst Immobilization without Covalent Attachment. *Green Chem.* **2021**, *23*, 4980–5005. [CrossRef]

14. Santos, J.C.S.D.; Barbosa, O.; Ortiz, C.; Berenguer-Murcia, A.; Rodrigues, R.C.; Fernandez-Lafuente, R. Importance of the Support Properties for Immobilization or Purification of Enzymes. *ChemCatChem* **2015**, *7*, 2413–2432. [CrossRef]

15. Garcia-Galan, C.; Berenguer-Murcia, Á.; Fernandez-Lafuente, R.; Rodrigues, R.C. Potential of Different Enzyme Immobilization Strategies to Improve Enzyme Performance. *Adv. Synth. Catal.* **2011**, *353*, 2885–2904. [CrossRef]

16. Bonet-Aleta, J.; Calzada-Funes, J.; Hueso, J.L. Recent Developments of Iron-Based Nanosystems as Enzyme-Mimicking Surrogates of Interest in Tumor Microenvironment Treatment. In *Nanomaterials for Biocatalysis*; Elsevier: Amsterdam, The Netherlands, 2022; pp. 237–265, ISBN 9780128244364.

17. Chen, Q.; Ma, X.; Xie, L.; Chen, W.; Xu, Z.; Song, E.; Zhu, X.; Song, Y. Iron-Based Nanoparticles for MR Imaging-Guided Ferroptosis in Combination with Photodynamic Therapy to Enhance Cancer Treatment. *Nanoscale* **2021**, *13*, 4855–4870. [CrossRef]

18. Bae, C.; Kim, H.; Kook, Y.M.; Lee, C.; Kim, C.; Yang, C.; Park, M.H.; Piao, Y.; Koh, W.G.; Lee, K. Induction of Ferroptosis Using Functionalized Iron-Based Nanoparticles for Anti-Cancer Therapy. *Mater. Today Bio* **2022**, *17*, 100457. [CrossRef]

19. Wang, L.L.; Fan, M.; Xing, X.; Liu, Y.; Sun, S. Immobilization of Glyceraldehyde-3-Phosphate Dehydrogenase on Fe_3O_4 Magnetic Nanoparticles and Its Application in Histamine Removal. *Colloids Surf. B Biointerfaces* **2021**, *205*, 111917. [CrossRef]

20. Monteiro, R.R.C.; Neto, D.M.A.; Fechine, P.B.A.; Lopes, A.A.S.; Gonçalves, L.R.B.; Dos Santos, J.C.S.; de Souza, M.C.M.; Fernandez-Lafuente, R. Ethyl Butyrate Synthesis Catalyzed by Lipases A and B from Candida Antarctica Immobilized onto Magnetic Nanoparticles. Improvement of Biocatalysts' Performance under Ultrasonic Irradiation. *Int. J. Mol. Sci.* **2019**, *20*, 5807. [CrossRef]

21. Khan, M.R. Immobilized Enzymes: A Comprehensive Review. *Bull. Natl. Res. Cent.* **2021**, *45*, 1–13. [CrossRef]

22. Hlady, V.; Buijs, J. Protein Adsorption on Solid Surfaces. *Curr. Opin. Biotechnol.* **1996**, *7*, 72–77. [CrossRef] [PubMed]

23. Rabe, M.; Verdes, D.; Seeger, S. Understanding Protein Adsorption Phenomena at Solid Surfaces. *Adv. Colloid Interface Sci.* **2011**, *162*, 87–106. [CrossRef] [PubMed]

24. Nakanishi, K.; Sakiyama, T.; Imamura, K. On the Adsorption of Proteins on Solid Surfaces, a Common but Very Complicated Phenomenon. *J. Biosci. Bioeng.* **2001**, *91*, 233–244. [CrossRef] [PubMed]

25. Rodrigues, R.C.; Ortiz, C.; Berenguer-Murcia, Á.; Torres, R.; Fernández-Lafuente, R. Modifying Enzyme Activity and Selectivity by Immobilization. *Chem. Soc. Rev.* **2013**, *42*, 6290–6307. [CrossRef]

26. Rodrigues, R.C.; Berenguer-Murcia, Á.; Carballares, D.; Morellon-Sterling, R.; Fernandez-Lafuente, R. Stabilization of Enzymes via Immobilization: Multipoint Covalent Attachment and Other Stabilization Strategies. *Biotechnol. Adv.* **2021**, *52*, 107821. [CrossRef]

27. Barbosa, O.; Ortiz, C.; Berenguer-Murcia, Á.; Torres, R.; Rodrigues, R.C.; Fernandez-Lafuente, R. Strategies for the One-Step Immobilization–Purification of Enzymes as Industrial Biocatalysts. *Biotechnol. Adv.* **2015**, *33*, 435–456. [CrossRef]

28. Sampaio, C.S.; Angelotti, J.A.F.; Fernandez-Lafuente, R.; Hirata, D.B. Lipase Immobilization via Cross-Linked Enzyme Aggregates: Problems and Prospects—A Review. *Int. J. Biol. Macromol.* **2022**, *215*, 434–449. [CrossRef]

29. Batool, I.; Iqbal, A.; Imran, M.; Ramzan, M.; Anwar, A. Design and Applications of Enzyme-Linked Nanostructured Materials for Efficient Bio-Catalysis. *Top. Catal.* **2023**, *66*, 649–675. [CrossRef]

30. Tsumoto, K.; Ejima, D.; Senczuk, A.M.; Kita, Y.; Arakawa, T. Effects of Salts on Protein–Surface Interactions: Applications for Column Chromatography. *J. Pharm. Sci.* **2007**, *96*, 1677–1690. [CrossRef]

31. Hall, J.B.; Dobrovolskaia, M.A.; Patri, A.K.; McNeil, S.E. Characterization of Nanoparticles for Therapeutics. *Nanomedicine* **2007**, *2*, 789–803. [CrossRef]

32. Slowing, I.I.; Vivero-Escoto, J.L.; Wu, C.W.; Lin, V.S.Y. Mesoporous Silica Nanoparticles as Controlled Release Drug Delivery and Gene Transfection Carriers. *Adv. Drug Deliv. Rev.* **2008**, *60*, 1278–1288. [CrossRef] [PubMed]

33. Bohunicky, B.; Mousa, S.A. Biosensors: The New Wave in Cancer Diagnosis. *Nanotechnol. Sci. Appl.* **2011**, *4*, 1–10.

34. Chen, H.; Yuan, L.; Song, W.; Wu, Z.; Li, D. Biocompatible Polymer Materials: Role of Protein-Surface Interactions. *Prog. Polym. Sci.* **2008**, *33*, 1059–1087. [CrossRef]

35. Zhou, H.; Mayorga-Martinez, C.C.; Pané, S.; Zhang, L.; Pumera, M. Magnetically Driven Micro and Nanorobots. *Chem. Rev.* **2021**, *121*, 4999–5041. [CrossRef]

36. Wang, L.; Meng, Z.; Chen, Y.; Zheng, Y. Engineering Magnetic Micro/Nanorobots for Versatile Biomedical Applications. *Adv. Intell. Syst.* **2021**, *3*, 2000267. [CrossRef]

37. Zhang, B.; Pan, H.; Chen, Z.; Yin, T.; Zheng, M.; Cai, L. Twin-Bioengine Self-Adaptive Micro/Nanorobots Using Enzyme Actuation and Macrophage Relay for Gastrointestinal Inflammation Therapy. *Sci. Adv.* **2023**, *9*, eadc8978. [CrossRef]

38. Walker, D.; Käsdorf, B.T.; Jeong, H.H.; Lieleg, O.; Fischer, P. Biomolecules: Enzymatically Active Biomimetic Micropropellers for the Penetration of Mucin Gels. *Sci. Adv.* **2015**, *1*, e1500501. [CrossRef]

39. Pan, H.; Qin, M.; Meng, W.; Cao, Y.; Wang, W. How Do Proteins Unfold upon Adsorption on Nanoparticle Surfaces? *Langmuir* **2012**, *28*, 12779–12787. [CrossRef]

40. Larsericsdotter, H.; Oscarsson, S.; Buijs, J. Structure, Stability, and Orientation of BSA Adsorbed to Silica. *J. Colloid Interface Sci.* **2005**, *289*, 26–35. [CrossRef]

41. Vertegel, A.A.; Richard, W.; Siegel, A.; Dordick, J.S. Silica Nanoparticle Size Influences the Structure and Enzymatic Activity of Adsorbed Lysozyme. *Langmuir* **2004**, *20*, 6800–6807. [CrossRef]

42. Wei, Y.; Thyparambil, A.A.; Wu, Y.; Latour, R.A. Adsorption-Induced Changes in Ribonuclease A Structure and Enzymatic Activity on Solid Surfaces. *Langmuir* **2014**, *30*, 14849–14858. [CrossRef] [PubMed]

43. Larsericsdotter, H.; Oscarsson, S.; Buijs, J. Thermodynamic Analysis of Proteins Adsorbed on Silica Particles: Electrostatic Effects. *J. Colloid Interface Sci.* **2001**, *237*, 98–103. [CrossRef] [PubMed]

44. Felsovalyi, F.; Mangiagalli, P.; Bureau, C.; Kumar, S.K.; Banta, S. Reversibility of the Adsorption of Lysozyme on Silica. *Langmuir* **2011**, *27*, 11873–11882. [CrossRef] [PubMed]

45. Linse, S.; Cabaleiro-Lago, C.; Xue, W.-F.; Lynch, I.; Lindman, S.; Thulin, E.; Radford, S.E.; Dawson, K.A. Nucleation of Protein Fibrillation by Nanoparticles. *Proc. Natl. Acad. Sci. USA* **2007**, *104*, 8691–8696. [CrossRef]

46. Daly, S.M.; Przybycien, T.M.; Tilton, R.D. Aggregation of Lysozyme and of Poly(Ethylene Glycol)-Modified Lysozyme after Adsorption to Silica. *Colloids Surf. B Biointerfaces* **2007**, *57*, 81–88. [CrossRef]

47. Liu, D.M.; Dong, C. Recent Advances in Nano-Carrier Immobilized Enzymes and Their Applications. *Process Biochem.* **2020**, *92*, 464–475. [CrossRef]

48. Netto, C.G.C.M.; Toma, H.E.; Andrade, L.H. Superparamagnetic Nanoparticles as Versatile Carriers and Supporting Materials for Enzymes. *J. Mol. Catal. B Enzym.* **2013**, *85–86*, 71–92. [CrossRef]

49. Bolivar, J.M.; Woodley, J.M.; Fernandez-Lafuente, R. Is Enzyme Immobilization a Mature Discipline? Some Critical Considerations to Capitalize on the Benefits of Immobilization. *Chem. Soc. Rev.* **2022**, *51*, 6251–6290. [CrossRef]

50. Bosio, V.E.; Islan, G.A.; Martínez, Y.N.; Durán, N.; Castro, G.R. Nanodevices for the Immobilization of Therapeutic Enzymes. *Crit. Rev. Biotechnol.* **2016**, *36*, 447–464. [CrossRef]

51. Rossi, L.M.; Costa, N.J.S.; Silva, F.P.; Wojcieszak, R. Magnetic Nanomaterials in Catalysis: Advanced Catalysts for Magnetic Separation and Beyond. *Green Chem.* **2014**, *16*, 2906–2933. [CrossRef]

52. Armenia, I.; Grazú Bonavia, M.V.; De Matteis, L.; Ivanchenko, P.; Martra, G.; Gornati, R.; de la Fuente, J.M.; Bernardini, G. Enzyme Activation by Alternating Magnetic Field: Importance of the Bioconjugation Methodology. *J. Colloid Interface Sci.* **2019**, *537*, 615–628. [CrossRef] [PubMed]

53. Ovejero, J.G.; Armenia, I.; Serantes, D.; Veintemillas-Verdaguer, S.; Zeballos, N.; López-Gallego, F.; Grüttner, C.; De La Fuente, J.M.; del Puerto Morales, M.; Grazu, V. Selective Magnetic Nanoheating: Combining Iron Oxide Nanoparticles for Multi-Hot-Spot Induction and Sequential Regulation. *Nano Lett.* **2021**, *21*, 7213–7220. [CrossRef] [PubMed]

54. Bonet-Aleta, J.; Sancho-Albero, M.; Calzada-Funes, J.; Irusta, S.; Martin-Duque, P.; Hueso, J.L.; Santamaria, J. Glutathione-Triggered Catalytic Response of Copper-Iron Mixed Oxide Nanoparticles. Leveraging Tumor Microenvironment Conditions for Chemodynamic Therapy. *J. Colloid Interface Sci.* **2022**, *617*, 704–717. [CrossRef] [PubMed]

55. Wei, H.; Wang, E. Fe_3O_4 Magnetic Nanoparticles as Peroxidase Mimetics and Their Applications in H2O2 and Glucose Detection. *Anal. Chem.* **2008**, *80*, 2250–2254. [CrossRef] [PubMed]

56. Wang, N.; Zhu, L.; Wang, D.; Wang, M.; Lin, Z.; Tang, H. Sono-Assisted Preparation of Highly-Efficient Peroxidase-like Fe_3O_4 Magnetic Nanoparticles for Catalytic Removal of Organic Pollutants with H2O2. *Ultrason. Sonochem.* **2010**, *17*, 526–533. [CrossRef]

57. Rocher, V.; Siaugue, J.-M.; Cabuil, V.; Bee, A. Removal of Organic Dyes by Magnetic Alginate Beads. *Water Res.* **2008**, *42*, 1290–1298. [CrossRef]

58. Yoon, T.-J.; Lee, W.; Oh, Y.-S.; Lee, J.-K. Magnetic Nanoparticles as a Catalyst Vehicle for Simple and Easy RecyclingElectronic Supplementary Information (ESI) Available: XRD and FT-IR Data, as Well as the Detailed Experimental Conditions for the Catalytic Hydroformylation Reactions. *New J. Chem.* **2003**, *27*, 227–229. [CrossRef]

59. Estelrich, J.; Sánchez-Martín, M.J.; Busquets, M.A. Nanoparticles in Magnetic Resonance Imaging: From Simple to Dual Contrast Agents. *Int. J. Nanomed.* **2015**, *10*, 1727–1741. [CrossRef]

60. Tartaj, P.; del Puerto Morales, M.; Veintemillas-Verdaguer, S.; González-Carreño, T.; Serna, C.J. The Preparation of Magnetic Nanoparticles for Applications in Biomedicine. *J. Phys. D. Appl. Phys.* **2003**, *36*, R182–R197. [CrossRef]

61. De Jong, W.H.; Borm, P.J.A. Drug Delivery and Nanoparticles:Applications and Hazards. *Int. J. Nanomed.* **2008**, *3*, 133–149. [CrossRef]

62. Sun, Z.-X.; Su, F.-W.; Forsling, W.; Samskog, P.-O. Surface Characteristics of Magnetite in Aqueous Suspension. *J. Colloid Interface Sci.* **1998**, *197*, 151–159. [CrossRef] [PubMed]

63. Derjaguin, B.; Landau, L. Theory of the Stability of Strongly Charged Lyophobic Sols and of the Adhesion of Strongly Charged Particles in Solutions of Electrolytes. *Prog. Surf. Sci.* **1993**, *43*, 30–59. [CrossRef]

64. Verwey, E.J.W. Theory of the Stability of Lyophobic Colloids. *J. Phys. Colloid Chem.* **1947**, *51*, 631–636. [CrossRef] [PubMed]

65. Tadros, T. Electrostatic and Steric Stabilization of Colloidal Dispersions. In *Electrical Phenomena at Interfaces and Biointerfaces*; John Wiley & Sons, Inc.: Hoboken, NJ, USA, 2012; pp. 153–172, ISBN 9781118135440.

66. Lu, A.-H.; Salabas, E.L.; Schüth, F. Magnetic Nanoparticles: Synthesis, Protection, Functionalization, and Application. *Angew. Chem. Int. Ed.* **2007**, *46*, 1222–1244. [CrossRef] [PubMed]

67. Smith, R.M.; Martell, A.E. *Critical Stability Constants*; Springer: Berlin/Heidelberg, Germany, 1989.

68. Kovář, D.; Malá, A.; Mlčochová, J.; Kalina, M.; Fohlerová, Z.; Hlaváček, A.; Farka, Z.; Skládal, P.; Starčuk, Z.; Jiřík, R.; et al. Preparation and Characterisation of Highly Stable Iron Oxide Nanoparticles for Magnetic Resonance Imaging. *J. Nanomater.* **2017**, *2017*, 7859289. [CrossRef]

69. Sahoo, Y.; Goodarzi, A.; Swihart, M.T.; Ohulchanskyy, T.Y.; Kaur, N.; Furlani, E.P.; Prasad, P.N. Aqueous Ferrofluid of Magnetite Nanoparticles: Fluorescence Labeling and Magnetophoretic Control. *J. Phys. Chem. B* **2005**, *109*, 3879–3885. [CrossRef]

70. Miguel-Sancho, N.; Bomatí-Miguel, O.; Colom, G.; Salvador, J.P.; Marco, M.P.; Santamaría, J. Development of Stable, Water-Dispersible, and Biofunctionalizable Superparamagnetic Iron Oxide Nanoparticles. *Chem. Mater.* **2011**, *23*, 2795–2802. [CrossRef]

71. Gorrepati, E.A.; Wongthahan, P.; Raha, S.; Fogler, H.S. Silica Precipitation in Acidic Solutions: Mechanism, PH Effect, and Salt Effect. *Langmuir* **2010**, *26*, 10467–10474. [CrossRef]

72. Bergna, H.E.; Roberts, W.O. *Colloidal Silica: Fundamentals and Applications*; CRC Taylor & Francis: Boca Raton, FL, USA, 2006; ISBN 9780824709679.

73. Liu, X.; Ma, Z.; Xing, J.; Liu, H. Preparation and Characterization of Amino–Silane Modified Superparamagnetic Silica Nanospheres. *J. Magn. Magn. Mater.* **2004**, *270*, 1–6. [CrossRef]

74. Shiraishi, Y.; Nishimura, G.; Hirai, T.K. Separation of Transition Metals Using Inorganic Adsorbents Modified with Chelating Ligands. *Ind. Eng. Chem. Res.* **2002**, *41*, 5065–5070. [CrossRef]

75. Malvindi, M.A.; De Matteis, V.; Galeone, A.; Brunetti, V.; Anyfantis, G.C.; Athanassiou, A.; Cingolani, R.; Pompa, P.P. Toxicity Assessment of Silica Coated Iron Oxide Nanoparticles and Biocompatibility Improvement by Surface Engineering. *PLoS ONE* **2014**, *9*, e85835. [CrossRef] [PubMed]

76. Stöber, W.; Fink, A.; Bohn, E. Controlled Growth of Monodisperse Silica Spheres in the Micron Size Range. *J. Colloid Interface Sci.* **1968**, *26*, 62–69. [CrossRef]

77. Lewandowska, J.; Staszewska, M.; Kepczynski, M.; Szuwarzyński, M.; Łatkiewicz, A.; Olejniczak, Z.; Nowakowska, M. Sol–Gel Synthesis of Iron Oxide–Silica Composite Microstructures. *J. Sol Gel Sci. Technol.* **2012**, *64*, 67–77. [CrossRef]

78. Bolivar, J.M.; Rocha-Martin, J.; Mateo, C.; Cava, F.; Berenguer, J.; Fernandez-Lafuente, R.; Guisan, J.M. Coating of Soluble and Immobilized Enzymes with Ionic Polymers: Full Stabilization of the Quaternary Structure of Multimeric Enzymes. *Biomacromolecules* **2009**, *10*, 742–747. [CrossRef] [PubMed]

79. Peng, M.; Li, H.; Luo, Z.; Kong, J.; Wan, Y.; Zheng, L.; Zhang, Q.; Niu, H.; Vermorken, A.; Van de Ven, W.; et al. Dextran-Coated Superparamagnetic Nanoparticles as Potential Cancer Drug Carriers in Vivo. *Nanoscale* **2015**, *7*, 11155–11162. [CrossRef]

80. Kalkan, N.A.; Aksoy, S.; Aksoy, E.A.; Hasirci, N. Preparation of Chitosan-Coated Magnetite Nanoparticles and Application for Immobilization of Laccase. *J. Appl. Polym. Sci.* **2012**, *123*, 707–716. [CrossRef]

81. Castelló, J.; Gallardo, M.; Busquets, M.A.; Estelrich, J. Chitosan (or Alginate)-Coated Iron Oxide Nanoparticles: A Comparative Study. *Colloids Surf. A Physicochem. Eng. Asp.* **2015**, *468*, 151–158. [CrossRef]

82. Chastellain, M.; Petri, A.; Hofmann, H. Particle Size Investigations of a Multistep Synthesis of PVA Coated Superparamagnetic Nanoparticles. *J. Colloid Interface Sci.* **2004**, *278*, 353–360. [CrossRef]

83. Butterworth, M.; Illum, L.; Davis, S. Preparation of Ultrafine Silica- and PEG-Coated Magnetite Particles. *Colloids Surf. A Physicochem. Eng. Asp.* **2001**, *179*, 93–102. [CrossRef]

84. Virgen-Ortíz, J.J.; Dos Santos, J.C.S.; Berenguer-Murcia, Á.; Barbosa, O.; Rodrigues, R.C.; Fernandez-Lafuente, R. Polyethylenimine: A Very Useful Ionic Polymer in the Design of Immobilized Enzyme Biocatalysts. *J. Mater. Chem. B* **2017**, *5*, 7461–7490. [CrossRef]

85. Barrat, J.-L.; Joanny, F. *Theory of Polyelectrolyte Solutions*; Wiley-Blackwell: Hoboken, NJ, USA, 2007; pp. 1–66.

86. Manning, G.S. Limiting Laws and Counterion Condensation in Polyelectrolyte Solutions I. Colligative Properties. *J. Chem. Phys.* **1969**, *51*, 924–933. [CrossRef]

87. Visakh, P.M. Polyelectrolyte: Thermodynamics and Rheology. In *Polyelectrolytes. Engineering Materials*; Visakh, P.M., Bayraktar, O., Picó, G., Eds.; Springer: Cham, Switzerland, 2014; pp. 1–17.

88. Drifford, M.; Delsanti, M. Polyelectrolyte Solutions with Multivalent Added Salts: Stability, Structure, and Dynamics. In *Physical Chemistry of Polyelectrolytes*; Marcel Dekker: New York, NY, USA, 2001; pp. 135–162, ISBN 9780824704636.

89. Kokufuta, E.; Takahashi, K. Adsorption of Poly(Diallyldimethylammonium Chloride) on Colloid Silica from Water and Salt Solution. *Macromolecules* **1986**, *19*, 351–354. [CrossRef]

90. Zhong, L.; Feng, Y.; Wang, G.; Wang, Z.; Bilal, M.; Lv, H.; Jia, S.; Cui, J. Production and Use of Immobilized Lipases in/on Nanomaterials: A Review from the Waste to Biodiesel Production. *Int. J. Biol. Macromol.* **2020**, *152*, 207–222. [CrossRef] [PubMed]

91. Lau, E.C.H.T.; Yiu, H.H.P. Enzyme Immobilization on Magnetic Nanoparticle Supports for Enhanced Separation and Recycling of Catalysts. In *Nanomaterials for Biocatalysis*; Elsevier: Amsterdam, The Netherlands, 2022; pp. 301–321, ISBN 9780128244364.

92. Roth, H.C.; Schwaminger, S.P.; Peng, F.; Berensmeier, S. Immobilization of Cellulase on Magnetic Nanocarriers. *ChemistryOpen* **2016**, *5*, 183–187. [CrossRef]

93. Lundqvist, M.; Ingmar Sethson, A. Bengt-Harald Jonsson Protein Adsorption onto Silica Nanoparticles: Conformational Changes Depend on the Particles' Curvature and the Protein Stability. *Langmuir* **2004**, *20*, 10639–10647. [CrossRef] [PubMed]

94. Andersson, M.M.; Hatti-Kaul, R. Protein Stabilising Effect of Polyethyleneimine. *J. Biotechnol.* **1999**, *72*, 21–31. [CrossRef]

95. Padilla-Martínez, S.G.; Martínez-Jothar, L.; Sampedro, J.G.; Tristan, F.; Pérez, E. Enhanced Thermal Stability and PH Behavior of Glucose Oxidase on Electrostatic Interaction with Polyethylenimine. *Int. J. Biol. Macromol.* **2015**, *75*, 453–459. [CrossRef]

96. Godbey, W.T.; Wu, K.K.; Mikos, A.G. Poly(Ethylenimine) and Its Role in Gene Delivery. *J. Control. Release* **1999**, *60*, 149–160. [CrossRef]

97. Ó'Fágáin, C. Enzyme Stabilization—Recent Experimental Progress. *Enzyme Microb. Technol.* **2003**, *33*, 137–149. [CrossRef]

98. Costa, S.A.; Tzanov, T.; Filipa Carneiro, A.; Paar, A.; Gübitz, G.M.; Cavaco-Paulo, A. Studies of Stabilization of Native Catalase Using Additives. *Enzyme Microb. Technol.* **2002**, *30*, 387–391. [CrossRef]

99. Singh, V.; Kaul, S.; Singla, P.; Kumar, V.; Sandhir, R.; Chung, J.H.; Garg, P.; Singhal, N.K. Xylanase Immobilization on Magnetite and Magnetite Core/Shell Nanocomposites Using Two Different Flexible Alkyl Length Organophosphonates: Linker Length and Shell Effect on Enzyme Catalytic Activity. *Int. J. Biol. Macromol.* **2018**, *115*, 590–599. [CrossRef] [PubMed]

100. Nematian, T.; Shakeri, A.; Salehi, Z.; Saboury, A.A. Lipase Immobilized on Functionalized Superparamagnetic Few-Layer Graphene Oxide as an Efficient Nanobiocatalyst for Biodiesel Production from Chlorella Vulgaris Bio-Oil. *Biotechnol. Biofuels* **2020**, *13*, 1–15. [CrossRef]

101. Ansari, S.A.; Husain, Q. Potential Applications of Enzymes Immobilized on/in Nano Materials: A Review. *Biotechnol. Adv.* **2012**, *30*, 512–523. [CrossRef] [PubMed]

102. Liu, D.M.; Chen, J.; Shi, Y.P. Advances on Methods and Easy Separated Support Materials for Enzymes Immobilization. *TrAC Trends Anal. Chem.* **2018**, *102*, 332–342. [CrossRef]

103. Zucca, P.; Fernandez-Lafuente, R.; Sanjust, E. Agarose and Its Derivatives as Supports for Enzyme Immobilization. *Molecules* **2016**, *21*, 1577. [CrossRef] [PubMed]

104. Cui, J.; Sun, B.; Lin, T.; Feng, Y.; Jia, S. Enzyme Shielding by Mesoporous Organosilica Shell on Fe_3O_4@silica Yolk-Shell Nanospheres. *Int. J. Biol. Macromol.* **2018**, *117*, 673–682. [CrossRef]

105. Homaei, A.A.; Sariri, R.; Vianello, F.; Stevanato, R. Enzyme Immobilization: An Update. *J. Chem. Biol.* **2013**, *6*, 185. [CrossRef]

106. Vaghari, H.; Jafarizadeh-Malmiri, H.; Mohammadlou, M.; Berenjian, A.; Anarjan, N.; Jafari, N.; Nasiri, S. Application of Magnetic Nanoparticles in Smart Enzyme Immobilization. *Biotechnol. Lett.* **2016**, *38*, 223–233. [CrossRef]

107. Estrella, V.; Chen, T.; Lloyd, M.; Wojtkowiak, J.; Cornnell, H.H.; Ibrahim-Hashim, A.; Bailey, K.; Balagurunathan, Y.; Rothberg, J.M.; Sloane, B.F.; et al. Acidity Generated by the Tumor Microenvironment Drives Local Invasion. *Cancer Res.* **2013**, *73*, 1524. [CrossRef]

108. Hlady, V.; Buijs, J.; Jennissen, H.P. [26] Methods for Studying Protein Adsorption. *Methods Enzymol.* **1999**, *309*, 402–429. [CrossRef]

109. Langmuir, I. The Adsorption of Gases on Plane Surfaces of Glass, Mica and Platinum. *J. Am. Chem. Soc.* **1918**, *40*, 1361–1403. [CrossRef]

110. Kipling, J.J. Adsorption from Partially Miscible Liquids. In *Adsorption from Solutions of Non-Electrolytes*; Elsevier: Amsterdam, The Netherlands, 1965; pp. 70–85, ISBN 9781483231068.

111. Andrade, J.D.; Hlady, V. Protein Adsorption and Materials Biocompatibility: A Tutorial Review and Suggested Hypotheses. In *Advances in Polymer Science*; Springer: Berlin/Heidelberg, Germany, 1986; pp. 1–63.

112. Izquierdo, J.F. *Cinética de Las Reacciones Químicas*; Edicions Universitat de Barcelona: Barcelona, Spain, 2004; ISBN 8483384795.

113. Kim, J.-H.; Yoon, J.-Y. Protein Adsorption On Polymer Particles. In *Encyclopedia of Surface and Colloid Science*; Marcel Dekker, Inc: New York, NY, USA, 2002.

114. Ding, C.; Ma, X.; Yao, X.; Jia, L. Facile Synthesis of Copper(II)-Decorated Magnetic Particles for Selective Removal of Hemoglobin from Blood Samples. *J. Chromatogr. A* **2015**, *1424*, 18–26. [CrossRef] [PubMed]

115. Wang, J.; Tan, S.; Liang, Q.; Guan, H.; Han, Q.; Ding, M. Selective Separation of Bovine Hemoglobin Using Magnetic Mesoporous Rare-Earth Silicate Microspheres. *Talanta* **2019**, *204*, 792–801. [CrossRef] [PubMed]

116. Kamran, S.; Absalan, G.; Asadi, M. A Comparative Study for Adsorption of Lysozyme from Aqueous Samples onto Fe_3O_4 Magnetic Nanoparticles Using Different Ionic Liquids as Modifier. *Amino Acids* **2015**, *47*, 2483–2493. [CrossRef] [PubMed]

117. Arai, K.; Murata, S.; Wang, T.; Yoshimura, W.; Oda-Tokuhisa, M.; Matsunaga, T.; Kisailus, D.; Arakaki, A. Adsorption of Biomineralization Protein Mms6 on Magnetite (Fe_3O_4) Nanoparticles. *Int. J. Mol. Sci.* **2022**, *23*, 5554. [CrossRef]

118. Carvalho, T.; Pereira, A.d.S.; Bonomo, R.C.F.; Franco, M.; Finotelli, P.V.; Amaral, P.F.F. Simple Physical Adsorption Technique to Immobilize Yarrowia Lipolytica Lipase Purified by Different Methods on Magnetic Nanoparticles: Adsorption Isotherms and Thermodynamic Approach. *Int. J. Biol. Macromol.* **2020**, *160*, 889–902. [CrossRef]

119. Kannan, K.; Mukherjee, J.; Mishra, P.; Gupta, M.N. Nickel Ferrite Nanoparticles as an Adsorbent for Immobilized Metal Affinity Chromatography of Proteins. *J. Chromatogr. Sci.* **2021**, *59*, 262–268. [CrossRef]
120. Chen, J.; Lin, Y.; Jia, L. Preparation of Anionic Polyelectrolyte Modified Magnetic Nanoparticles for Rapid and Efficient Separation of Lysozyme from Egg White. *J. Chromatogr. A* **2015**, *1388*, 43–51. [CrossRef]
121. Namdeo, M.; Bajpai, S.K. Enzymatic Immobilization of a-Amylase onto Cellulose-Coated Magnetite (CCM) Nanoparticles and Preliminary Starch Degradation Study. *J. Mol. Catal. B* **2009**, *59*, 134–139. [CrossRef]
122. Pogorilyi, R.P.; Melnyk, I.V.; Zub, Y.L.; Seisenbaeva, G.A.; Kessler, V.G.; Shcherbatyik, M.M.; Košak, A.; Lobnik, A. Urease Adsorption and Activity on Magnetite Nanoparticles Functionalized with Monofunctional and Bifunctional Surface Layers. *J. Sol Gel Sci. Technol.* **2013**, *68*, 447–454. [CrossRef]
123. Gal, N.; Schroffenegger, M.; Reimhult, E. Stealth Nanoparticles Grafted with Dense Polymer Brushes Display Adsorption of Serum Protein Investigated by Isothermal Titration Calorimetry. *J. Phys. Chem. B* **2018**, *122*, 5820–5834. [CrossRef] [PubMed]
124. Zhao, T.; Chen, K.; Gu, H. Investigations on the Interactions of Proteins with Polyampholyte-Coated Magnetite Nanoparticles. *J. Phys. Chem. B* **2013**, *117*, 14129–14135. [CrossRef] [PubMed]
125. Leitner, N.S.; Schroffenegger, M.; Reimhult, E. Polymer Brush-Grafted Nanoparticles Preferentially Interact with Opsonins and Albumin. *ACS Appl. Bio Mater.* **2021**, *4*, 795–806. [CrossRef] [PubMed]
126. Tapdiqov, S.Z.; Ambrosio, L.; Raucci, M.G. Adsorption of Trypsin Onto Ph Sensitive Poly-N-Vinylpyyrolidone-Co-Poly-4-Vinylpyridine and Its Magnetic Based Hydrogel: Sorption Isotherms and Thermodynamic Parameters. *SSRN Electron. J.* **2023**, *357*, 114371. [CrossRef]
127. Muley, A.B.; Mulchandani, K.H.; Singhal, R.S. Immobilization of Enzymes on Iron Oxide Magnetic Nanoparticles: Synthesis, Characterization, Kinetics and Thermodynamics. *Methods Enzymol.* **2020**, *630*, 39–79. [CrossRef]
128. Ahmed, S.A.; Saleh, S.A.A.; Abdel-Hameed, S.A.M.; Fayad, A.M. Catalytic, Kinetic and Thermodynamic Properties of Free and Immobilized Caseinase on Mica Glass-Ceramics. *Heliyon* **2019**, *5*, e01674. [CrossRef]
129. Bindu, V.U.; Mohanan, P.V. Thermal Deactivation of α-Amylase Immobilized Magnetic Chitosan and Its Modified Forms: A Kinetic and Thermodynamic Study. *Carbohydr. Res.* **2020**, *498*, 108185. [CrossRef]
130. Wong, W.K.L.; Wahab, R.A.; Onoja, E. Chemically Modified Nanoparticles from Oil Palm Ash Silica-Coated Magnetite as Support for Candida Rugosa Lipase-Catalysed Hydrolysis: Kinetic and Thermodynamic Studies. *Chem. Pap.* **2020**, *74*, 1253–1265. [CrossRef]
131. Mohammadi, M.; Rezaei Mokarram, R.; Ghorbani, M.; Hamishehkar, H. Inulinase Immobilized Gold-Magnetic Nanoparticles as a Magnetically Recyclable Biocatalyst for Facial and Efficient Inulin Biotransformation to High Fructose Syrup. *Int. J. Biol. Macromol.* **2019**, *123*, 846–855. [CrossRef]
132. Desai, R.P.; Dave, D.; Suthar, S.A.; Shah, S.; Ruparelia, N.; Kikani, B.A. Immobilization of α-Amylase on GO-Magnetite Nanoparticles for the Production of High Maltose Containing Syrup. *Int. J. Biol. Macromol.* **2021**, *169*, 228–238. [CrossRef]
133. Verma, M.L.; Chaudhary, R.; Tsuzuki, T.; Barrow, C.J.; Puri, M. Immobilization of β-Glucosidase on a Magnetic Nanoparticle Improves Thermostability: Application in Cellobiose Hydrolysis. *Bioresour. Technol.* **2013**, *135*, 2–6. [CrossRef] [PubMed]
134. Onoja, E.; Chandren, S.; Razak, F.I.A.; Wahab, R.A. Enzymatic Synthesis of Butyl Butyrate by Candida Rugosa Lipase Supported on Magnetized-Nanosilica from Oil Palm Leaves: Process Optimization, Kinetic and Thermodynamic Study. *J. Taiwan Inst. Chem. Eng.* **2018**, *91*, 105–118. [CrossRef]
135. Fortes, C.C.S.; Daniel-da-Silva, A.L.; Xavier, A.M.R.B.; Tavares, A.P.M. Optimization of Enzyme Immobilization on Functionalized Magnetic Nanoparticles for Laccase Biocatalytic Reactions. *Chem. Eng. Process. Process Intensif.* **2017**, *117*, 1–8. [CrossRef]
136. Savitha, D.P.; Bindu, V.U.; Geetha, G.; Mohanan, P. V Improvement in the Properties of α-Amylase Enzyme by Immobilization Using Metal Oxide Nanocomposites as Carriers. *Adv. Nanomed. Nanotechnol. Res.* **2020**, *2*, 77–88.
137. Jacob, A.G.; Wahab, R.A.; Misson, M. Operational Stability, Regenerability, and Thermodynamics Studies on Biogenic Silica/Magnetite/Graphene Oxide Nanocomposite-Activated Candida Rugosa Lipase. *Polymer* **2021**, *13*, 3854. [CrossRef]
138. Barbosa, O.; Torres, R.; Ortiz, C.; Berenguer-Murcia, Á.; Rodrigues, R.C.; Fernandez-Lafuente, R. Heterofunctional Supports in Enzyme Immobilization: From Traditional Immobilization Protocols to Opportunities in Tuning Enzyme Properties. *Biomacromolecules* **2013**, *14*, 2433–2462. [CrossRef]
139. Torres-Salas, P.; Del Monte-Martinez, A.; Cutiño-Avila, B.; Rodriguez-Colinas, B.; Alcalde, M.; Ballesteros, A.O.; Plou, F.J. Immobilized Biocatalysts: Novel Approaches and Tools for Binding Enzymes to Supports. *Adv. Mater.* **2011**, *23*, 5275–5282. [CrossRef]
140. Gkantzou, E.; Chatzikonstantinou, A.V.; Fotiadou, R.; Giannakopoulou, A.; Patila, M.; Stamatis, H. Trends in the Development of Innovative Nanobiocatalysts and Their Application in Biocatalytic Transformations. *Biotechnol. Adv.* **2021**, *51*, 107738. [CrossRef]
141. Mehrasbi, M.R.; Mohammadi, J.; Peyda, M.; Mohammadi, M. Covalent Immobilization of Candida Antarctica Lipase on Core-Shell Magnetic Nanoparticles for Production of Biodiesel from Waste Cooking Oil. *Renew. Energy* **2017**, *101*, 593–602. [CrossRef]
142. Kharazmi, S.; Taheri-Kafrani, A.; Soozanipour, A. Efficient Immobilization of Pectinase on Trichlorotriazine-Functionalized Polyethylene Glycol-Grafted Magnetic Nanoparticles: A Stable and Robust Nanobiocatalyst for Fruit Juice Clarification. *Food Chem.* **2020**, *325*, 126890. [CrossRef]
143. Kempe, H.; Kempe, M. The Use of Magnetite Nanoparticles for Implant-Assisted Magnetic Drug Targeting in Thrombolytic Therapy. *Biomaterials* **2010**, *31*, 9499–9510. [CrossRef] [PubMed]

144. Marques da Silva, M.; Wanderley Duarte Neto, J.M.; Barros Regueira, B.V.; Torres do Couto, M.T.; Vitória da Silva Sobral, R.; Sales Conniff, A.E.; Pedrosa Brandão Costa, R.M.; Cajubá de Britto Lira Nogueira, M.; Pereira da Silva Santos, N.; Pastrana, L.; et al. Immobilization of Fibrinolytic Protease from Mucor Subtilissimus UCP 1262 in Magnetic Nanoparticles. *Protein Expr. Purif.* **2022**, *192*, 106044. [CrossRef] [PubMed]

145. Aber, S.; Mahmoudikia, E.; Karimi, A.; Mahdizadeh, F. Immobilization of Glucose Oxidase on Fe$_3$O$_4$ Magnetic Nanoparticles and Its Application in the Removal of Acid Yellow 12. *Water. Air. Soil Pollut.* **2016**, *227*, 93. [CrossRef]

146. Betancor, L.; Fuentes, M.; Dellamora-Ortiz, G.; López-Gallego, F.; Hidalgo, A.; Alonso-Morales, N.; Mateo, C.; Guisán, J.M.; Fernández-Lafuente, R. Dextran Aldehyde Coating of Glucose Oxidase Immobilized on Magnetic Nanoparticles Prevents Its Inactivation by Gas Bubbles. *J. Mol. Catal. B Enzym.* **2005**, *32*, 97–101. [CrossRef]

147. Mahmood, I.; Ahmad, I.; Chen, G.; Huizhou, L. A Surfactant-Coated Lipase Immobilized in Magnetic Nanoparticles for Multicycle Ethyl Isovalerate Enzymatic Production. *Biochem. Eng. J.* **2013**, *73*, 72–79. [CrossRef]

148. Wang, J.; Li, K.; He, Y.; Wang, Y.; Han, X.; Yan, Y. Enhanced Performance of Lipase Immobilized onto Co^{2+}-Chelated Magnetic Nanoparticles and Its Application in Biodiesel Production. *Fuel* **2019**, *255*, 115794. [CrossRef]

149. Barkoula, N.M.; Alcock, B.; Cabrera, N.O.; Peijs, T. Flame-Retardancy Properties of Intumescent Ammonium Poly(Phosphate) and Mineral Filler Magnesium Hydroxide in Combination with Graphene. *Polym. Polym. Compos.* **2008**, *16*, 101–113. [CrossRef]

150. Chen, S.C.; Sheu, D.C.; Duan, K.J. Production of Fructooligosaccharides Using β-Fructofuranosidase Immobilized onto Chitosan-Coated Magnetic Nanoparticles. *J. Taiwan Inst. Chem. Eng.* **2014**, *45*, 1105–1110. [CrossRef]

151. Atacan, K.; Çakiroğlu, B.; Özacar, M. Improvement of the Stability and Activity of Immobilized Trypsin on Modified Fe$_3$O$_4$ Magnetic Nanoparticles for Hydrolysis of Bovine Serum Albumin and Its Application in the Bovine Milk. *Food Chem.* **2016**, *212*, 460–468. [CrossRef]

152. Alam, S.; Nagpal, T.; Singhal, R.; Kumar Khare, S. Immobilization of L-Asparaginase on Magnetic Nanoparticles: Kinetics and Functional Characterization and Applications. *Bioresour. Technol.* **2021**, *339*, 125599. [CrossRef]

153. Xiao, Q.; Liu, C.; Ni, H.; Zhu, Y.; Jiang, Z.; Xiao, A. β-Agarase Immobilized on Tannic Acid-Modified Fe$_3$O$_4$ Nanoparticles for Efficient Preparation of Bioactive Neoagaro-Oligosaccharide. *Food Chem.* **2019**, *272*, 586–595. [CrossRef]

154. Xue, K.; Liu, C.L.; Yang, Y.; Liu, X.; Zhan, J.; Bai, Z. Immobilization of D-Allulose 3-Epimerase into Magnetic Metal–Organic Framework Nanoparticles for Efficient Biocatalysis. *World J. Microbiol. Biotechnol.* **2022**, *38*, 1–11. [CrossRef] [PubMed]

155. Abdulaal, W.H.; Almulaiky, Y.Q. Encapsulation of HRP Enzyme onto a Magnetic Fe$_3$O$_4$ Np—PMMA Film via Casting with Sustainable. *Biocatal. Act.* **2020**, *10*, 181. [CrossRef]

156. Zanker, A.A.; Ahmad, N.; Son, T.H.; Schwaminger, S.P.; Berensmeier, S. Selective Ene-Reductase Immobilization to Magnetic Nanoparticles through a Novel Affinity Tag. *Biotechnol. J.* **2021**, *16*, e2000366. [CrossRef] [PubMed]

157. Fauser, J.; Savitskiy, S.; Fottner, M.; Trauschke, V.; Gulen, B. Sortase-Mediated Quantifiable Enzyme Immobilization on Magnetic Nanoparticles. *Bioconjug. Chem.* **2020**, *31*, 1883–1892. [CrossRef]

158. Pan, C.; Hu, B.; Li, W.; Sun, Y.; Ye, H.; Zeng, X. Novel and Efficient Method for Immobilization and Stabilization of β-d-Galactosidase by Covalent Attachment onto Magnetic Fe$_3$O$_4$–Chitosan Nanoparticles. *J. Mol. Catal. B Enzym.* **2009**, *61*, 208–215. [CrossRef]

159. Tuncagil, S.; Kayahan, S.K.; Bayramoglu, G.; Arica, M.Y.; Toppare, L. L-Dopa Synthesis Using Tyrosinase Immobilized on Magnetic Beads. *J. Mol. Catal. B Enzym.* **2009**, *58*, 187–193. [CrossRef]

160. Sun, C.; Lee, J.S.H.; Zhang, M. Magnetic Nanoparticles in MR Imaging and Drug Delivery. *Adv. Drug Deliv. Rev.* **2008**, *60*, 1252–1265. [CrossRef]

161. Zhou, Z.; Yang, L.; Gao, J.; Chen, X. Structure–Relaxivity Relationships of Magnetic Nanoparticles for Magnetic Resonance Imaging. *Adv. Mater.* **2019**, *31*, 1804567. [CrossRef]

162. Liu, X.; Zhang, Y.; Wang, Y.; Zhu, W.; Li, G.; Ma, X.; Zhang, Y.; Chen, S.; Tiwari, S.; Shi, K.; et al. Comprehensive Understanding of Magnetic Hyperthermia for Improving Antitumor Therapeutic Efficacy. *Theranostics* **2020**, *10*, 3793–3815. [CrossRef]

163. Mou, X.; Ali, Z.; Li, S.; He, N. Applications of Magnetic Nanoparticles in Targeted Drug Delivery System. *J. Nanosci. Nanotechnol.* **2015**, *15*, 54–62. [CrossRef] [PubMed]

164. El-Boubbou, K. Magnetic Iron Oxide Nanoparticles as Drug Carriers: Preparation, Conjugation and Delivery. *Nanomedicine* **2018**, *13*, 929–952. [CrossRef]

165. Zhang, L.; Li, C.X.; Wan, S.S.; Zhang, X.Z. Nanocatalyst-Mediated Chemodynamic Tumor Therapy. *Adv. Healthc. Mater.* **2022**, *11*, 2101971. [CrossRef] [PubMed]

166. Mbakidi, J.P.; Drogat, N.; Granet, R.; Ouk, T.S.; Ratinaud, M.H.; Rivière, E.; Verdier, M.; Sol, V. Hydrophilic Chlorin-Conjugated Magnetic Nanoparticles—Potential Anticancer Agent for the Treatment of Melanoma by PDT. *Bioorg. Med. Chem. Lett.* **2013**, *23*, 2486–2490. [CrossRef] [PubMed]

167. Ni, D.; Ferreira, C.A.; Barnhart, T.E.; Quach, V.; Yu, B.; Jiang, D.; Wei, W.; Liu, H.; Engle, J.W.; Hu, P.; et al. Magnetic Targeting of Nanotheranostics Enhances Cerenkov Radiation-Induced Photodynamic Therapy. *J. Am. Chem. Soc.* **2018**, *140*, 14971–14979. [CrossRef] [PubMed]

168. Xu, Z.; Chen, J.; Li, Y.; Hu, T.; Fan, L.; Xi, J.; Han, J.; Guo, R. Yolk-Shell Fe$_3$O$_4$@Carbon@Platinum-Chlorin E6 Nanozyme for MRI-Assisted Synergistic Catalytic-Photodynamic-Photothermal Tumor Therapy. *J. Colloid Interface Sci.* **2022**, *628*, 1033–1043. [CrossRef] [PubMed]

169. Chen, T.; Chu, Q.; Li, M.; Han, G.; Li, X. Fe$_3$O$_4$@Pt Nanoparticles to Enable Combinational Electrodynamic/Chemodynamic Therapy. *J. Nanobiotechnol.* **2021**, *19*, 1–13. [CrossRef]

170. Yu, G.T.; Rao, L.; Wu, H.; Yang, L.L.; Bu, L.L.; Deng, W.W.; Wu, L.; Nan, X.; Zhang, W.F.; Zhao, X.Z.; et al. Myeloid-Derived Suppressor Cell Membrane-Coated Magnetic Nanoparticles for Cancer Theranostics by Inducing Macrophage Polarization and Synergizing Immunogenic Cell Death. *Adv. Funct. Mater.* **2018**, *28*, 1801389. [CrossRef]

171. Cao, W.; Jin, M.; Yang, K.; Chen, B.; Xiong, M.; Li, X.; Cao, G. Fenton/Fenton-like Metal-Based Nanomaterials Combine with Oxidase for Synergistic Tumor Therapy. *J. Nanobiotechnol.* **2021**, *19*, 1–35. [CrossRef]

172. Fu, L.H.; Qi, C.; Lin, J.; Huang, P. Catalytic Chemistry of Glucose Oxidase in Cancer Diagnosis and Treatment. *Chem. Soc. Rev.* **2018**, *47*, 6454–6472. [CrossRef]

173. Huo, M.; Wang, L.; Chen, Y.; Shi, J. Tumor-Selective Catalytic Nanomedicine by Nanocatalyst Delivery. *Nat. Commun.* **2017**, *8*, 357. [CrossRef] [PubMed]

174. Wu, J.; Ma, S.; Li, M.; Hu, X.; Jiao, N.; Tung, S.; Liu, L. Enzymatic/Magnetic Hybrid Micromotors for Synergistic Anticancer Therapy. *ACS Appl. Mater. Interfaces* **2021**, *13*, 31514–31526. [CrossRef] [PubMed]

175. Qin, X.; Wu, C.; Niu, D.; Qin, L.; Wang, X.; Wang, Q.; Li, Y. Peroxisome Inspired Hybrid Enzyme Nanogels for Chemodynamic and Photodynamic Therapy. *Nat. Commun.* **2021**, *12*, 5243. [CrossRef] [PubMed]

176. Ashtari, K.; Khajeh, K.; Fasihi, J.; Ashtari, P.; Ramazani, A.; Vali, H. Silica-Encapsulated Magnetic Nanoparticles: Enzyme Immobilization and Cytotoxic Study. *Int. J. Biol. Macromol.* **2012**, *50*, 1063–1069. [CrossRef]

177. Fuentes-Baile, M.; Pérez-Valenciano, E.; García-Morales, P.; de Juan Romero, C.; Bello-Gil, D.; Barberá, V.M.; Rodríguez-Lescure, Á.; Sanz, J.M.; Alenda, C.; Saceda, M. Clyta-Daao Chimeric Enzyme Bound to Magnetic Nanoparticles. A New Therapeutical Approach for Cancer Patients? *Int. J. Mol. Sci.* **2021**, *22*, 1477. [CrossRef]

178. Zhang, F.; Li, H.; Liu, C.; Fang, K.; Jiang, Y.; Wu, M.; Xiao, S.; Zhu, L.; Yu, J.; Li, S.; et al. Lactate Dehydrogenase-Inhibitors Isolated from Ethyl Acetate Extract of Selaginella Doederleinii by Using a Rapid Screening Method with Enzyme-Immobilized Magnetic Nanoparticles. *Front. Biosci. Landmark* **2022**, *27*, 229. [CrossRef]

179. Zhou, J.; Zhang, J.; Gao, W. Enhanced and Selective Delivery of Enzyme Therapy to 9L-Glioma Tumor via Magnetic Targeting of PEG-Modified, β-Glucosidase-Conjugated Iron Oxide Nanoparticles. *Int. J. Nanomed.* **2014**, *9*, 2905–2917. [CrossRef]

180. Mu, X.; Qiao, J.; Qi, L.; Dong, P.; Ma, H. Poly(2-Vinyl-4,4-Dimethylazlactone)-Functionalized Magnetic Nanoparticles as Carriers for Enzyme Immobilization and Its Application. *ACS Appl. Mater. Interfaces* **2014**, *6*, 21346–21354. [CrossRef]

181. Orhan, H.; Aktaş Uygun, D. Immobilization of L-Asparaginase on Magnetic Nanoparticles for Cancer Treatment. *Appl. Biochem. Biotechnol.* **2020**, *191*, 1432–1443. [CrossRef]

182. Zhang, T.; Li, Y.; Hong, W.; Chen, Z.; Peng, P.; Yuan, S.; Qu, J.; Xiao, M.; Xu, L. Glucose Oxidase and Polydopamine Functionalized Iron Oxide Nanoparticles: Combination of the Photothermal Effect and Reactive Oxygen Species Generation for Dual-Modality Selective Cancer Therapy. *J. Mater. Chem. B* **2019**, *7*, 2190–2200. [CrossRef]

183. Zhang, Y.; Wang, Y.; Zhou, Q.; Chen, X.; Jiao, W.; Li, G.; Peng, M.; Liu, X.; He, Y.; Fan, H. Precise Regulation of Enzyme-Nanozyme Cascade Reaction Kinetics by Magnetic Actuation toward Efficient Tumor Therapy. *ACS Appl. Mater. Interfaces* **2021**, *13*, 52395–52405. [CrossRef] [PubMed]

184. Fuentes-Baile, M.; Bello-Gil, D.; Pérez-Valenciano, E.; Sanz, J.M.; García-Morales, P.; Maestro, B.; Ventero, M.P.; Alenda, C.; Barberá, V.M.; Saceda, M. CLytA-DAAO, Free and Immobilized in Magnetic Nanoparticles, Induces Cell Death in Human Cancer Cells. *Biomolecules* **2020**, *10*, 222. [CrossRef] [PubMed]

185. Jiang, S.; Chen, X.; Lin, J.; Huang, P. Lactate-Oxidase-Instructed Cancer Diagnosis and Therapy. *Adv. Mater.* **2023**, *35*, 2207951. [CrossRef] [PubMed]

186. Bian, H.; Sun, B.; Cui, J.; Ren, S.; Lin, T.; Feng, Y.; Jia, S. Bienzyme Magnetic Nanobiocatalyst with Fe^{3+}-Tannic Acid Film for One-Pot Starch Hydrolysis. *J. Agric. Food Chem.* **2018**, *66*, 8753–8760. [CrossRef]